



Fluorous Drug-Affinity Proteomics for Cancer Drug Discovery

Citation

Herzberg, Benjamin. 2015. Fluorous Drug-Affinity Proteomics for Cancer Drug Discovery. Doctoral dissertation, Harvard Medical School.

Link

<http://nrs.harvard.edu/urn-3:HUL.InstRepos:15821582>

Terms of use

This article was downloaded from Harvard University's DASH repository, and is made available under the terms and conditions applicable to Other Posted Material (LAA), as set forth at

<https://harvardwiki.atlassian.net/wiki/external/NGY5NDE4ZjgzNTc5NDQzMGIzZWZhMGFIOWI2M2EwYTg>

Accessibility

<https://accessibility.huit.harvard.edu/digital-accessibility-policy>

Share Your Story

The Harvard community has made this article openly available.
Please share how this access benefits you. [Submit a story](#)

Abstract

Identifying the intracellular targets of small molecules – target ID – is a major problem in chemical biology with broad application to the discovery and development of novel therapies. Traditional target ID studies have relied on drug-affinity chromatography to separate biological mixtures combined with mass spectrometry shotgun sequencing for peptide identification. This workflow is limited, however, by low specificity for unique peptides, high demand for cellular material, unknown depth of profiling, and other problems. To address these problems, we explore and describe here a novel strategy for cell lysis and drug-affinity that we call “fluorous proteomics.” By conjugating a small molecule to a perfluorinated alkane, we hypothesized that we could achieve superior recovery, specificity, and identification, allowing us to identify previously unknown drug targets with drug-affinity methods. We establish the conditions for fluorous proteomics and synthesize fluorinated probes for two drugs as a proof-of-concept. Lenalidomide, a derivative of thalidomide with unknown intracellular targets but widespread clinical use, is investigated and novel binders are identified. A particular derivative, 5HPP33, is singled out for potential future drug development. JQ1, an inhibitor of BET bromodomains in development as a treatment for hematological malignancies, is used to compare biotinylated versus fluorous tags and to identify new binders of possible therapeutic relevance. We conclude that fluorous proteomics retains high potential as an alternative to traditional drug-affinity chromatography strategies and may aid in target ID going forward, but is not without complications.

Table of Contents

Fluorous drug-affinity proteomics for cancer drug discovery.....	1
Abstract	2
Introduction.....	6
Genomics and drug discovery	6
Target identification	7
Chemical proteomics and drug-affinity chromatography.....	9
Fluorous proteomics for target ID	11
Lenalidomide and target ID.....	13
JQ1 and target ID.....	16
Materials and Methods	17
Reagents.....	17
Cell culture and functional studies.....	17
Synthetic chemistry	18
Cell lysis and protein extraction	19
Assessment of protein activities.....	20
Western Blot	20
Drug affinity chromatography.....	21
Protein purification	21
Peptide mass spectrometry, identification and quantitation	22

Zebrafish drug treatment experiments.....	23
Results.....	24
Selection of proof-of-method problems for fluorous proteomics.....	24
Lenalidomide has cell-autonomous tumor activity.....	24
Testing of other thalidomide derivatives establishes an SAR and identifies derivatives for further development.....	25
5HPP33 as a potential lead for drug development and Target ID	27
Lenalidomide in a zebrafish model.....	28
Synthesis and testing of a lenalidomide-fluorous probe.....	29
Establishing experimental conditions for fluorous proteomics	30
Fluorous proteomics of lenalidomide	32
JQ1 in T-ALL	34
Biotinylated JQ1 drug-affinity chromatography	35
Fluorous proteomics of JQ1.....	35
Discussion.....	37
Summary	37
The mechanism of lenalidomide	38
Difficulties (and possible successes) with fluorous proteomics	39
Acknowledgments.....	41
Figures and Tables	42

References..... 51

Introduction

Genomics and drug discovery

It is commonly asserted that genomics and other high-throughput technologies have revolutionized the practice of biology, and that they offer the surest way forward for understanding and treating many of our most pressing medical concerns – diseases such as diabetes, cancer, HIV, autoimmune disorders, and more (Collins *et al.*, 2003). Yet the post-genomic explosion of data in biology has, by at least one measure, been resolutely resistant to practical application in the clinic: the yearly approval of new drugs has stayed the same or markedly declined in the last fifteen years (Horrobin 2001; Milne, 2003). Drug discovery, an inherently stochastic and slow process, has simply not kept up with the exponential growth seen elsewhere in this “revolution” of the biological sciences.

This is not to say that there have not been major successes in deploying new drugs in the clinic. Targeted therapies such as Gleevec (Bucdunger *et al.*, 1996; Druker *et al.*, 1996) and biologicals such as bevacizumab, to name just two well-known cancer treatments that came to market in the last fifteen years, have brought many more previously-refractory diseases under the heading of “treatable.” Still, the new targeted or “rationally designed” therapies have not escaped the old Achilles heels of resistance (especially with quick-evolving targets like cancer cells or some viruses) or off-target effects (Quintas-Cardama *et al.*, 2007). Considering that there are perhaps hundreds of thousands of different expressed proteins, splice isoforms, post-translational modifications, and mutants – it is estimated that there are 3,000 to 10,000 druggable targets in the human proteome (Overington *et al.*, 2006) – the fact that only roughly 500 proteins are currently exploited by a drug in any form is remarkable (Meisner *et al.*, 2004). Even in a disease with a putatively well-established target, the preclinical data that leads to investigatory drug development can sometimes be misleading (Begley and Ellis, 2012), and extremely careful, direct

validation of targets is required beyond the circumstantial evidence that is often supplied in the literature from single experiments (Prinz *et al.*, 2011). At the same time, once a target is well-validated, screens of hundreds of thousands of compounds can fail to yield any notable hits – perhaps because we do not capture the full chemical space (Hert *et al.*, 2009) – though some progress has been made in chemical diversification of libraries (Schreiber, 2000). However much of a role is played by any of these specific limitations of biology or chemistry, the relative poverty of drug development is beginning to look particularly glaring when one can, for instance, enumerate to a patient the entirety of the mutation spectrum in their tumor and yet lack even a single chemical entity to hit any of the targets the sequencing presents. Innovation in the discovery of new drugs is now, perhaps for the first time, the major bottleneck to current medical progress in a large number of diseases.

Target identification

The first step in most projects of drug discovery is the search for a druggable target, such as might be implied by the mutations present in tumor DNA or the proteins packaged in a virus. The next step is an attempt to find a molecule which hits that target. Flipping this problem over, once in possession of a biologically active compound, we may not know all of the proteins to which it binds in a cell. This knowledge is crucial for understanding side-effect profiles, pharmacokinetics, further drug development, and more. The discovery of mechanistically-relevant *targets* for in-hand *compounds* is generally termed the problem of drug “target identification.”

Target ID may be performed on compounds of unknown or known medical effects. In the case of small molecules with unknown or merely suspected clinical relevance, target ID may be performed as a follow-up to hits on phenotypic screens (Bredel and Jacoby, 2004), or for investigation based on chemical similarity to known drugs (Savchuk *et al.*, 2004 Schuffenhauer *et al.*, 2003), or as a part of drug derivatization for investigational or medical use (Frye, 2010). Computer modeling and structural

chemistry can play a key role (Laggner *et al.*, 2011), and innovative approaches combining proteomics, computation, and molecular biology are consistently being applied (see for instance Wacker *et al.*, 2012). Where drugs have known therapeutic utility but unknown cellular targets, target ID can have additional implications. A drug with a known use (say as an empirically-derived malaria treatment) can be employed to identify a novel protein target (perhaps a protein critical to parasite invasion), thus spurring new drug development (structurally similar drugs for the same target, or new screens). That same drug may be used to identify promiscuous binding to other proteins that may generate side-effects, paving the way for new development to reduce this off-target binding, or even utilize off target effects for further avenues of development. Protein complexes can be purified and new targets with the same mechanistic principles can be pursued (inhibiting different members of a transcriptional complex, for instance). Thus target ID on compounds of known medical use can leverage chemical biology for the discovery of new biological knowledge, new lines of drug development, and new clinical information – all at once.

Remarkably, given the paucity of successful targeted therapies, a significant number of drugs that *are* actively prescribed in a clinical setting in fact have no known cellular targets. Two influential reviews have argued that somewhere between 7 (Drews, 2000) and 21 (Overington *et al.*, 2006) percent of all FDA-approved drugs have no known primary target or mechanism of action, even while they have clearly demonstrated therapeutic value. This estimate may be, to a certain extent, an exaggeration or an easily-remedied quirk of the methods most commonly employed in drug discovery (Gregori-Puigjane *et al.*, 2012), but it is nonetheless clear that in a strikingly large number of cases, we lack complete information about which intracellular targets of a clinically-relevant small molecule are therapeutically relevant, which generate side-effects, and which are merely hangers-on. Importantly, this problem is not limited to a single disease, or single class of molecules: drugs with unknown directly-bound targets include Halofantrine, an anti-malarial; antibiotics such as 4-aminosalicylic acid (TB) and clofazimine (leprosy); anesthetics such as halothane and diethyl ether (the oldest known!); the now-widely-used anti-

convulsant levetiracetam (Keppra); and even the diabetes drug metformin, though some advances have been made in elucidating its mechanism (Miller *et al.*, 2012) has few known direct binders (Imming 2006).

Chemical proteomics and drug-affinity chromatography

Target ID for known medical compounds is therefore a major biological and clinical problem as well as a unique opportunity. Classically, several methods have been employed for the discovery of drug targets: activity-based probe profiling, which focuses particularly on the activity of a protein family in response to a drug (Jaeger *et al.*, 2004; Barglow and Cravatt, 2007); analysis of changes in cellular composition due to drug treatment, such as by microarray or proteomics (see for instance Eggert *et al.*, 2004; Kuruvilla *et al.*, 2002); and compound-centric chemical proteomics, which consists of traditional drug affinity chromatography to purify and identify drug-binding molecules (reviewed in Rix and Furga, 2009). Drug-affinity chromatography methods have been used for target ID for decades with significant success (Cuatrecasas *et al.*, 1970; Harding *et al.*, 1989; Sabatini *et al.*, 1994). The essential idea of drug affinity proteomics is to extract a proteome from a cell lysate of interest, separate out the mixture based on affinity for the drug, bind the drug-protein complex to a stable matrix, wash away unbound proteins, elute, and identify peptides that bound the drug (Figure 1A). Innovations in drug chromatography have made it almost the procedure of choice for Target ID (Rix 2004). The identification of proteins has in particular benefited from the deployment of mass spectrometry (MS) techniques with higher sensitivity, through innovations such as nano-electrospray ionization (ESI) (Wilm and Mann, 1996), high-performance liquid chromatography (HPLC), and high resolution spectrometers (Hoffman, 2005). Combining these advances with stable isotope labeling (Ong *et al.*, 2002) or other tags (Aggarwal, *et al.*, 2006; Ross *et al.*, 2004) and the wide availability of protein databases and bioinformatics has led to more reliable quantification and identification. These advances have been used to greatly improve the

sensitivity of target drug discovery (Belcher *et al.*, 2012; Chen *et al.*, 2010). Target identification has been performed using LC-MS drug affinity chromatography for antibiotics (Schug *et al.*, 2011), kinase inhibitors (Bantscheff *et al.*, 2007; Brehmer *et al.*, 2004; Godl *et al.*, 2005; Rix *et al.*, 2007), and more.

While MS-based drug affinity experiments have several advantages – the identification is roughly unbiased, proteome-wide and requires only native cellular lysate – they have also been plagued by significant limitations. There is high demand for cellular material, and lysis conditions may not sample each compartment of the cell equally; conventional extraction methods often bias cytosolic protein recovery, and deeper profiling can necessitate the use of harsh reagents which can denature complexes and mask important protein-drug and protein-protein interactions (Vodisch *et al.*, 2009). There are sample throughput limitations, especially in the case of quantification and many non-specific binders. Non-specific interactions to the drug-affinity matrix are common and can confound results by washing out signals from proteins of more biological importance (Bantscheff *et al.*, 2011). The choice of matrix is in turn related to the choice of tag employed on the small molecule, which brings its own concerns. A tag or linker that is too large can interfere with native protein binding, while the chemical modulation of a drug required to tag it may alter its own chemical properties. So as to minimize these concerns, chemical derivatization must be carefully related to structural activity data, say from a structure-activity relationship series (SAR). An SAR may not always be rigorously known – and even when it is, chemical alteration of a drug may still involve guesswork. Finally, since recovery of material is proportional to *both* protein-drug affinity and protein abundance (Graves and Wu, 1974), high-affinity and biologically-important binders that are in low cellular abundance may be weak “hits” in a traditional screen due to this bias.

Fluorous proteomics for target ID

The combination of these deficiencies might be predicted to lead to significant “blind-spots” in drug-affinity chromatography target ID experiments. These blind spots might also go some length to explaining a deficiency in existing methods of drug discovery and development: if the most commonly used unbiased method to detect drug-protein interactions in the laboratory has methodological difficulties, all aspects of drug discovery and development are likely to be correspondingly more difficult.

Consequently, in the work presented here, we chose two cancer drugs – one in active use in the clinic and one in clinical development (with widespread use as a chemical probe) – and applied new method development for target ID as well as the initial steps of further drug discovery. In taking this approach, we hoped to demonstrate the feasibility of new technological applications to drug discovery-focused proteomics, as well as to use these new approaches on interesting drugs as a proof-of-concept. Our method development was focused on increasing the sensitivity and specificity of target ID. One of the major limitations of affinity chromatography, cited above, is excess binding of proteins to resin, linker, or other requirements of the experimental set up which depart from the normal *in vivo* environment of the drug-protein interaction. In nearly all experiments, small molecules of interest are conjugated, usually via long hydrophobic linker, to some tag which has specificity for a corresponding resin (see Figure 1A). The most commonly used tag-resin pair is a biotin tag and streptavidin resin, though this is by no means the only choice. Nearly all resins share in common, however, a descent from biological systems – streptavidin is itself a *protein* – and consequently they generate many non-specific protein interactions with the resin itself. The sheer weight of non-specific binders to such resins can overwhelm any signal from truly unique drug-protein interactions. We therefore began by searching for a resin which has suitable properties for drug-affinity chromatography – separation capabilities under

normal solvent conditions, suitably small tags, ease of chemical modification, etc. – which might also minimize non-specific interactions with the protein lysate.

We chose to investigate “fluorous tags.” Fluorous tags, which have been in use for several years in synthetic organic chemistry settings, make use of the unique properties of perfluorinated alkanes (Gladysz *et al.*, 2006). The motivation for fluorous chemistry is derived from the observation that perfluorinated solvents dissolve perfluorinated molecules better than either aqueous or organic solvents, while excluding non-fluorinated organic compounds and solvents – thus allowing for rapid purification and separation of a single compound in a synthetic setting (Dobbs and Kimberley, 2002). The initial use of fluorous chemistry was in “biphasic” systems (Horvath and Rabai, 1994), in which a reaction could occur in a “mixed phase” of fluorous and another liquid phase which had limited or no solubility in fluorous phases, such as organic solvents. While organic and fluorous phases readily intermixed at a certain temperature, they then resolved into two phases when cooled. This “in-between” property of fluorinated molecules allowed for reactions to occur at the fluorous phase or at the interface of the phases, but only the desired product was retained in the fluorous phase (or at least the two separated reaction products in a predictable manner, allowing one to choose which products of the reaction to carry forward).

The facile separation of products from reactants and catalysts under mild conditions initiated great interest in synthetic settings; soon the concept of a “ponytail” – which was eventually renamed a “fluorous tag” – evolved (Gladysz and Curran, 2002). In typical use, a molecule which commonly has normal organic reactivity – and is consequently soluble in conventional organic solvents – can be “tagged” with a perfluorinated alkane, which confers preferential solubility in fluorous phases but retains the reactivity of the original organic molecule. Synthetic reactions can be carried out, and, during extraction, a fluorous solvent can rapidly and easily purify only the fluorous molecule, just as in traditional biphasic fluorous systems (Zhang, 2006). This eliminates the need for complex fluorination

and allows for a predictable, modular approach to separation and reaction purification. Since its early uses, fluorine chemistry has evolved to include solid silica-based fluorinated phases for use in typical applications such as HPLC, solid-phase purification, microarray immobilization, and more.

Drawing inspiration from the use of fluorine chemistry in such synthetic settings, we hypothesized that a fluorine-tagged small molecule might be reliably recovered from a complex protein mixture by binding to the fluorine resin, thereby replicating the typical “biotinylated-compound/streptavidin resin” strategy employed in drug affinity chromatography. In addition to the ease of use and simplicity that such a method might have (this is the advantage which already increased its popularity in the synthetic organic chemistry setting), we also hypothesized that such a resin-linker combination might generate a much lower rate of non-specific effects due to the elimination of proteins or biological-like molecules (such as the common His tag) from the resin-tag pair. This in turn would greatly increase the specificity of target ID experiments. We call this approach “fluorine proteomics,” and employed it here for the investigation of two compounds of interest.

Lenalidomide and target ID

We chose two cancer drugs to test fluorine proteomics target ID: the multiple myeloma drug lenalidomide (revlimid) and the experimental bromodomain inhibitor JQ1. Lenalidomide is in current clinical use and in several clinical trials for an expanding sphere of indications. JQ1 is a first-in-class drug with widespread laboratory use as a probe and early investigation as both a cancer drug and contraceptive.

Lenalidomide, which is a derivative of thalidomide, is one of the so-called “immunomodulatory drugs” (IMiDs). Thalidomide, which was initially observed to have anti-inflammatory but T-cell boosting properties (from which it gets the IMiD label), is perhaps one of the most historically interesting drugs in recent medical history. It was widely prescribed as a sedative in the 1950s until it was

found to have grossly teratogenic properties, which engendered a scandal that birthed the modern form of the FDA. Judah Folkman identified thalidomide as an inhibitor of angiogenesis in 1994 (D'Amato *et al.*, 1994) after which it was tried as a myeloma drug and found to have significant efficacy in patients. A derivative of thalidomide with a single amine on the phthalimide group, known as lenalidomide, was found to increase the potency of thalidomide's anti-myeloma effect several fold *in vitro* and have increased efficacy *in vivo* as well (Palumbo *et al.*, 2012). A combination of glucocorticoid (prednisone or dexamethasone), proteasome inhibitors like bortezomib, and a thalidomide analog like lenalidomide is now commonly the frontline treatment for multiple myeloma (Palumbo *et al.*, 2010).

But no satisfactory consensus exists as to the mechanism of the anti-tumor effect of thalidomide analogs (Singhal *et al.*, 1999; Ching *et al.*, 2007) or an exact list of cellular targets they bind. The drug has known cell-autonomous effects on apoptosis (Hideshima *et al.*, 2000), but it is also anti-angiogenic (D'Amato *et al.*, 1994), alters extracellular matrix remodeling (Geitz *et al.*, 1996), suppresses production of tumor necrosis factor alpha while increasing IL-2 production (Sampaio *et al.*, 1991), and has a hand in changing expression and response to various other cytokines (Corral *et al.*, 1996; Haslett *et al.*, 1998). Thalidomide and its analogs have been reported to have clear cell-autonomous effects *in vitro*, but the dosage at which these effects takes place does not appear to be within the therapeutic concentration given to patients in simple models (Chung *et al.*, 2004). Thus significant questions about the mechanism of lenalidomide have long been part of its mystery.

Recently, both before and after this work was completed, significant strides have been made towards elucidating the mechanism of lenalidomide. When this work was initially started, the most well-known effect of thalidomide, its teratogenicity, had been traced to thalidomide's binding and inhibition of cereblon (CRBN) – a component of the E3 ubiquitin ligase complex – with subsequent modification of developmental pathways such as the down-regulation of fibroblast growth factors (Ito *et al.*, 2010). CRBN was identified as a binder of thalidomide in the original study by traditional target ID methods,

and downregulation of CRBN in zebrafish and chick models was found to mimic the effects of thalidomide in those species. Other work immediately following this connected CRBN with thalidomide's anti-tumor effect, but the evidence was indirect (Zhu *et al.*, 2011). Because of the close resemblance of thalidomide and lenalidomide, it was natural to hypothesize that CRBN did indeed underlie the effect and that target ID would identify it as a binder of lenalidomide as well. But lenalidomide is not nearly as teratogenic as thalidomide in previously tested models (Barlett *et al.*, 2004), implying some difference in mechanism between lenalidomide and thalidomide.

Since the work below was completed, the mechanism of lenalidomide has been fleshed out in novel and highly influential work which, in a way, proves the point that target ID can reveal novel biology as much as novel drug design. Two studies, using vastly different experimental designs, reported that lenalidomide does, in fact, bind cereblon in myeloma cell lines (Kronke *et al.*, 2014; Lu *et al.*, 2014). The binding of lenalidomide to cereblon initiates a selective and novel ubiquitination of two immune-cell development transcription factors from the Ikaros family, Ikaros (IKZF1) and Aiolos (IKZF3). After binding to cereblon in the presence of lenalidomide, these proteins are rapidly degraded, while other nearly-homologous members of the Ikaros family (IKZF2, 4 and 5) were unaffected, and selective mutation of certain residues in Ikaros and Aiolos to look more like other family members could abrogate the anti-proliferative effect of lenalidomide. Interestingly, both these transcription factors are critical for normal plasma cell development and loss of function mutations have been associated with acute lymphoblastic leukemia. IKZF loss also led to decreased expression of IRF4, which had been seen in prior experiments with lenalidomide (Yang *et al.*, 2012), and is a known repressor of IL-2, explaining lenalidomide's effect on other immune cells. These two papers therefore pointed to not only a novel mechanism of action for lenalidomide, but perhaps a novel mechanism of action in all of drug discovery: selectively altered ubiquitination. A further recent paper solved the crystal structure of CRBN-DDB1 in complex with lenalidomide, and could therefore lead to design programs aimed at hitting previously

“undruggable” targets by modulation of ubiquitination (Chamberlain *et al.*, 2014). While the solution to the lenalidomide mystery has therefore been by and large resolved, many questions remain, and some of the work presented below may still induce useful directions of investigation in this regard.

JQ1 and target ID

JQ1 – in contrast to lenalidomide – is not a widely used clinical drug but is a first-in-class inhibitor of the bromodomain and extra terminal (BET) family of proteins (Filippakopoulos *et al.*, 2010) which has widely reported potential in hematological malignancies. BET proteins, which act as “adaptors” on acetylated histones to recruit polymerases and activate transcription, have recently been identified as playing a major role in the pathogenesis of some cancers (Zuber *et al.*, 2011), and BET inhibition is a promising strategy for rewiring the transcriptional profile of many cell types to a quiescent state, leading to the investigation of JQ1 as a potential male contraceptive through the inhibition of sperm maturation (Matzuk *et al.*, 2012). The mechanism of JQ1 as an anti-cancer agent is novel, and likely involves a highly unique selective downregulation of the transcription of c-Myc, a well-known oncogene in many varieties of cancer, via a profound depletion of transcriptional machinery from “super-enhancer” sites in the genome (Lovén *et al.*, 2013).

The strongest protein binders of JQ1 are known, and JQ1 and other BET inhibitors have been used extensively as a chemical probe to find members of the histone reading complex (Dawson *et al.*, 2011). None of these experiments, however, have been as robust as an unbiased mass-spectrometry based screen. We therefore chose to investigate JQ1 because the robust proteomics data already available on JQ1 and similar drugs would allow a ready comparison between our technique and previously applied proteomics techniques. In addition, reports of new effects of JQ1 on various cancer cell lines are continually being produced (Ott *et al.*, 2012), and we generate data here for the first time on JQ1 treatment in leukemia cell lines in which JQ1 is reported to have unique effects.

Materials and Methods

Reagents

All reagents were of ACS grade, and obtained from Thermo Scientific, unless noted otherwise. Lenalidomide, pomalidomide, thalidomide, (+)-thalidomide, (-)-thalidomide, and 5HPP33 were obtained from Sigma-Aldrich. JQ1 was obtained from Jun Qi, Bradner lab. Stable isotope-labeled $^{15}\text{N}_2$, $^{13}\text{C}_6$ -lysine (K8) and $^{15}\text{N}_4$, $^{13}\text{C}_6$ -arginine (R10) and their natural abundance analogues were obtained from Cambridge Isotope Laboratories. Pluronic F-127, Octyl-beta glucoside and NDSB-195 were obtained from Santa Cruz. Fluorous silica resin (40um) was obtained from Fluorous Technologies.

Cell culture and functional studies

Cell lines were obtained from the German Collection of Microorganisms and Cell Cultures (Brunswick, Germany). All cells were cultured in RPMI-1640 medium supplemented with penicillin/streptomycin and 10% fetal bovine serum, with the exception of CD34 cells cultured in SFEM supplemented with cytokines cocktails CC110 and CC200 from Stemcell Technologies (Vancouver, Canada). Suspension and adherent cells were maintained at a density of 0.5-1 million cells/ml or 50-90% confluence, respectively, at 37 °C in a humidified atmosphere with 5% CO₂. For metabolic labeling, cells were cultured for 6 doubling times in RPMI-1640 supplemented with either light or heavy isotope-labeled lysine and arginine and 10% dialyzed fetal bovine serum (Thermo Scientific) and checked by LC-MS/MS for the presence of heavy labeled peptides. Cell counts were measured using the Neubauer hemocytometer (Hausser Scientific) or the Countess (Invitrogen) with Trypan Blue staining (Invitrogen) according to manufacturer's instructions.

Jurkat cells engineered to express GFP and KOPTK1 cells expressing shRNA targeting control GFP were generated by retroviral transduction as described (Cepko *et al.*, 2001).

For analysis of fluoruous lenalidomide cell penetration, cells were treated with fluoruous lenalidomide for 1 hour and immediately lysed in RIPA buffer supplemented by protease and phosphatase inhibitors (Sigma), and both media and cell fractions were qualitatively assessed for presence of lenalidomide in a TOF-LCT mass spectrometer coupled to a Waters 2690 LC and 2996 photoiodide detector (Waters, Milford, MA).

Cell growth kinetics were measured by seeding cells in a 96-well plate, 10,000 cells per well, with or without the presence of drug or DMSO control. Cell counts were obtained using CellTiter-Glo (Promega) at intervals of 1 or 4 days read as per instructions on a FLUOstar Omega microplate reader (BMG Labtech).

Synthetic chemistry

Biotinylated JQ1 and fluoruous JQ1 were obtained from Jason Marineau, Bradner Lab. An initial stock of fluoruous lenalidomide was also obtained from JJM.

For synthesis of a second generation fluoruous lenalidomide probe, lenalidomide (55mg, 0.212 mmol) was dissolved in THF with 47.687mg sodium iodide (1.5 eq, 0.318 mmol), 5.5992 mg NaH (1.1 eq, 0.2333 mmol) and 32.63mg 5-chloro-pentyne (1.5 eq, 0.3115 mmol) at 0.05M in 4.242mL THF. The reaction was quenched with saturated aqueous sodium bicarbonate and the aqueous layer extracted three times with ethyl acetate. Combined organic extracts were washed with brine, dried over sodium sulfate and concentrated, but failed to yield a significant fraction going forward unlike previous reports (Stewart *et al.*, 2010).

In a second attempt, 50mg of lenalidomide (0.1929 mol) was dissolved in 0.9409 mL of THF (0.05M). 117.62 mg of triethylamine (6eq, 1.1574 mmol), 0.47 mg of DMAP, and 50.5mg of di-tert-butyl dicarbonate (f-boc) (1.1 eq, 0.231mmol) were added to the reaction and allowed to stir overnight, after which an additional 15mg (0.3eq) f-boc was added empirically to the reaction mixture. The reaction was

quenched with ice and water and extracted twice with ethylacetate, water and brine. The previously attempted reaction was repeated with excess NaH (3eq) and run and extracted as previously described. The reaction was purified by HPLC with an eluting gradient of 0-100% methanol in dichloromethane and afforded 8mg of yellowish solid. At this point work was stopped on further synthesis of a second generation probe.

For the synthesis of additional fluoros lenalidomide, lenalidomide (50 mg, 0.193 mmol, 1.1 equivalent) was dissolved in dichloromethane (2.5 mL, 0.05 M). Perfluorooctylethylisocyanate (55 mg, 0.113 mmol, 1 equiv.) was added, followed by diisopropylethylamine (20 uL, 0.113 mmol, 1 equiv.). The reaction was stirred under an inert atmosphere for 18 hours and then concentrated. The residue was purified by fluoros solid phase extraction using a 2g/8cc FluoroFlash cartridge (Fluorous Technologies Inc., USA) equilibrated with 80:20 methanol:water (2 X 3 mL). The residue was loaded as a solution in 2 mL DMSO. The column was then washed with 80:20 methanol:water (2X3mL) and the fluoros product eluted with tetrahydrofuran (2 X 3 mL). The fluoros fraction was concentrated to afford 6 mg of a white solid.

Fluorous perphenazine, for proof of concept, was graciously provided by Alex Kenstis and Jason Marineau.

All reactions were followed on a Waters TOF-LCT MS coupled to Waters 2690 LC and Waters 2996 photoiodide detector.

Cell lysis and protein extraction

Harvested cells were washed once with cold phosphate-buffered saline, and frozen at -80 °C for 12 hours. Thawed cells were resuspended in cold 150 mM NaCl, 50 mM Tris-HCl, pH 7.5, supplemented with EDTA-free protease inhibitors (Roche) and 1% (v/v) detergents as indicated. For comparison of mechanical disruption methods, suspensions of 100 million cells in 1.8 ml of lysis buffer were processed

by using 20 strokes of the 2 ml Potter-Elvehjem homogenizer on ice (Corning) or disruption using the Covaris E210 adaptive focusing acoustic sonicator and 13x65 mm tubes operating in the frequency sweep mode at 1000 Hz, 20% duty cycle, and intensity 8 for 600 seconds at 4 °C, or incubation at 95 °C for 5 min in the lysis buffer supplemented with 1% SDS. All lysates were clarified by centrifugation at 16,000 *g* for 10 minutes at 4 °C. Protein concentration was measured using the bicinchoninic acid assay according to manufacturer's instructions, and read on at BioRad Benchmark Plus spectrophotometer plate reader.

Assessment of protein activities

For GFP-expressing cells, GFP activity was measured using fluorescence emission spectroscopy with excitation of 488 nm and emission at 530 nm using 96-well plates (200 uL lysate/well) and the FLUOstar Omega plate reader.

Western Blot

Anti-CRBN antibodies were obtained from ProteinTech (rabbit polyclonal, whole peptide) and Abcam (mouse polyclonal, amino acids 1-442; rabbit polyclonal, N-terminus 1-33) and used as per manufacturers instructions. Anti-rabbit and anti-mouse secondary antibodies conjugated with horseradish peroxidase were obtained from Thermo, and visualized using SuperSignal West Femto Chemiluminescent substrate, according to manufacturer's instructions (Thermo). Image densitometry was performed using ImageJ (NIH).

Drug affinity chromatography

Biotinylated JQ1 was immobilized using NeutrAvidin UltraLink resin (Thermo Scientific) by incubating 100 uL of resin slurry (0.005 umol of avidin) with 10uL of 10 mM solution of PPZ-biotin in DMSO (0.1 umol) and 900 uL of Lysis buffer with 1% (w/v) Pluronic F-127 and 1% (w/v) octyl-beta-glucoside (PO buffer) at room temperature for 30 minutes on shaking mixer. For fluorous affinity chromatography, 40 um FluoroFlash silica resin (Fluorous Technologies) was incubated in 80% aqueous methanol for 15 minutes at room temperature in a shaking mixer, and wetted resin was washed twice with PO buffer. Washed resin was then incubated with fluorous JQ1 or lenalidomide in PO buffer, and drug-bound resins were washed 5 times with PO buffer, added to 3-5mg of clarified cell lysates diluted to 1.8 ml final volume with PO buffer either in the presence of 500 uM free competitor drugs dissolved in DMSO (light isotope-labeled proteome) or DMSO alone (9% v/v, heavy isotope-labeled proteome), and incubated while rotating at 4 °C overnight. Protein-bound resin was washed 3 times with PO buffer, pooled to combine heavy and light-labeled fractions, and bound proteins were eluted by incubating resins in 0.2 ml of 8M urea, 50 mM Tris-HCl, pH 7.5 for 30 minutes at room temperature while on shaking mixer.

Protein purification

Urea-eluted proteins were purified by addition of 1 ml of cold chloroform:methanol (2:1) to extract residual detergent, and mixtures were centrifuged at 16,000 *g* for 15 minutes at 4 °C. Protein discs at the organic:aqueous interface were transferred to a new tube and washed with cold acetone. Alternatively, peptides were precipitated by addition of 400 uL methanol followed by 100 uL chloroform and 300 uL water. An additional 400 uL of methanol was added, lysates were cleared at 16,000*g* and the protein was washed twice with acetone. After drying, peptides were dissolved in 70 uL of 0.1% (w/v) RapiGest (Waters) in 50 mM ammonium bicarbonate, pH 8.5 (ABC buffer) by incubating for 30 minutes at 37 °C

while on a shaking mixer. Solubilized proteins were reduced with 5 mM dithiothreitol by incubation for 45 minutes at 56 °C, and alkylated with 15 mM iodoacetamide by incubation at room temperature for 30 minutes in the dark. Proteins were subsequently digested with 2 ug porcine trypsin (Promega) by incubation at 37 °C for 18 hours. RapiGest was removed by hydrolysis with 200 mM HCl at 37 °C for 45 minutes and centrifugation at 16,000 *g* for 20 minutes. Tryptic peptides were purified by reverse phase chromatography using C₁₈ SpinTips and 0.1% TFA wash, according to manufacturer's instructions (Nest Group), and concentrated using vacuum centrifugation.

Peptide mass spectrometry, identification and quantitation

Tryptic peptides were dissolved in 5% (v/v) aqueous acetonitrile and 0.1% (v/v) formic acid and were resolved and ionized using nanoflow HPLC (nanoLC, Eksigent) coupled to the LTQ or LTQ-Orbitrap hybrid mass spectrometer (Thermo). Nanoflow chromatography, electrospray ionization and data-dependent acquisition were performed as described, with the resolution of 60,000 and m/z range of 350-2000 (Kentsis, 2009). Recorded mass spectra were searched against the International Protein Index database (version 3.91) that included reverse decoy sequences by using the Andromeda algorithm as implemented in MaxQuant (version 1.0.13.13) (Cox, 2011) for heavy/light quantification or by ProteinPilot (Applied Biosystems) for peptide ID (also against IPI 3.91). Variable modifications for *N*-acetylation, methionine oxidation, and fixed cysteine carbamidomethylation were included. Mass tolerance for precursor and fragment ions was 10 ppm and 0.8 Da, respectively, with the false discovery rate of 1% at the peptide and protein levels. For quantitation, identified peptides were filtered to include only those with matched light and heavy isotope spectra, and peptide intensities were averaged for the highest ranking protein mappings to calculate relative abundances of light and heavy proteins, respectively. Gene Ontology (GO) annotations were computed using DAVID (version 6.7).

Zebrafish drug treatment experiments

Fish were kept at 28.5 °C on a 14-h light/10-h dark cycle, and embryos were obtained from the Look Lab as described previously (Etchin, 2011). For drug treatment, 10mM stock was added to a final concentration of 400-10uM thalidomide to 60-100 embryos in E3 medium. Zebrafish embryos were dechorionated prior to drug treatment at 6hpf by incubation in E3 medium containing 5mg/mL pronase (Sigma) for 3 minutes at room temperature, then washed five times with E3 medium. Embryos were immediately transferred to E3 medium containing drug. Every 6 hours during growth at 28.5 °C embryos were checked by light microscopy for morphogenic alterations as previously described (Ito *et al.*, 2010). At 75hpf embryos were fixed in 4% paraformaldehyde in PBS, washed with PBS, transferred to 100% methanol, and stored at -20°C overnight. When ready to be examined, embryos were immersed in 50% MeOH in PBST for five minutes, 30% MeOH for another 5%, rinsed, and fixed again for 20 minutes in PBS at RT. After rinsing, they were processed either for in-situ staining (not reported in this study) or simple examination (reported).

Results

Selection of proof-of-method problems for fluoruous proteomics

We wished to test novel methods in the isolation, purification, and identification of peptides via drug affinity chromatography. To do so, as described above, we searched for drugs of suitable interest to test our platform. The ideal drug would be of biological or clinical interest, have substantive outstanding questions about its intracellular binding profile, have some reported binders to serve as internal positive controls, and have relatively rich background chemical literature to establish a theoretical SAR which might be confirmed in our own experiments.

We settled on two drug-systems that we felt best fit these criteria: thalidomide analogs and bromodomain inhibitors such as JQ1. In both cases we performed a thorough review of the chemical literature, which included the establishment of a putative structure-activity relationship (SAR) for derivatives of thalidomide (see Table S1). The individual approaches to these drugs, combined with fluoruous proteomics development, are described below.

Lenalidomide has cell-autonomous tumor activity

We first investigated thalidomide analogs. The mechanism of action of thalidomide derivatives has been extensively discussed in the literature, but no consensus exists as to the exact biochemical genesis of the anti-tumor activity which makes this class so therapeutically valuable. This made it an ideal drug class with which to test innovations in target ID: there is a significant background literature of observed effects and widespread clinical use of the drug class, but no direct observations of protein-drug interactions through proteomic approaches. New derivatives are in clinical development with only slightly altered chemical properties (Lacy *et al.*, 2009; Lacy *et al.*, 2010), and the class has been extensively

investigated for immunological properties as well, leading to a large stable of chemical data (Miyachi *et al.*, 1997).

Before beginning to investigate thalidomide, we wanted to verify for ourselves the anti-proliferative effects of thalidomide and its derivatives. We first tested lenalidomide, the most commonly used anti-myeloma drug, in a variety of myeloma and leukemia cell lines by treating cell lines for 1 to 4 days and observing inhibition of cell growth. At 1 day almost no growth inhibition was noted, so further experiments were carried out only at 4 days. The results are displayed in Figure 2A. Lenalidomide displayed an IC₅₀ ranging from 15-30uM in various cell lines, but did not reach full inhibition of cell growth at concentrations up to 50uM, consistent with many prior reports. At any higher concentrations, DMSO was observed to inhibit cell growth in our assay and confound any possible observed drug effects. Three cell lines – the dexamethasone-resistant myeloma cell line OPM1 and the leukemia cell lines KG-1 and HL-60 (Figure 2B) – showed no inhibition at any tested concentration, consistent with reports that lenalidomide's effect is cell-line specific. Of note, lenalidomide inhibition requires high doses of drug, and also has an odd inhibition profile – it does not show good specific inhibition, but rather a slow descent – both facts possibly implying a complicated basis for lenalidomide's inhibition of cell growth, making it a problem of specific interest for high-specificity proteomics. It also has a fairly high IC₅₀. We therefore decided to move forward with an investigation of thalidomide derivatives as a test of our strategy.

Testing of other thalidomide derivatives establishes an SAR and identifies derivatives for further development

Thalidomide has undergone extensive development and testing for a variety of interesting *in vitro* properties. Derivatives have been reported that have widely varying biological effects and efficacy with only small changes in overall chemical structure. To build a probe for target ID proteomics experiments

necessarily requires that a drug be chemically modified in some form by addition of a linker and tag. But not all positions on a drug are created equal, and some modifications are less disruptive to drug binding than others; thus careful attention to known differences between molecules with only slightly different chemical composition is critical to a successful target ID experiment. In addition, though thalidomide derivatives have been tested extensively for specific *in vitro* effects, much of the derivatization of thalidomide was done before thalidomide was a widely-used cancer treatment and was focused on other properties such as “immunomodulation”. Thus significant knowledge about thalidomide derivatives’ effects on myeloma lines as compared to currently used drugs is lacking in all but a few cases. Finally, in some assays, thalidomide’s effects are not seen unless thalidomide can be metabolized before reaching its target cell (Price *et al.*, 2002). Thalidomide metabolites, and not the drug itself, have therefore sometimes been considered the active species. One hypothesized metabolite in particular, 5-hydroxy-thalidomide, has been proposed as the active drug.

Therefore, to establish a SAR for thalidomide analogs biological effects, we tested a variety of thalidomide analogs for effects on the myeloma cell line MM1s. The structure of thalidomide analogs used is displayed in Figure 3A. Lenalidomide, discussed above, is the most widely used thalidomide derivative in a clinical setting. Pomalidomide, which is 4-amino-thalidomide (in the numbering scheme usually adopted in the literature; see Miyachi *et al.*, 1997) has promising activity in clinical trials and is sometimes reported to have a higher IC50 than lenalidomide. 5HPP33 is from a class of thalidomide-like molecules in which the glutaramide is replaced by a benzyl, which showed significant anti-inflammatory activity *in vitro*. Significant differences have sometimes been observed between the stereoisomers of thalidomide, though they readily convert *in vivo* (Teo *et al.*, 2003; Ito *et al.*, 2010). 5-OH-Thalidomide has already been mentioned as the potential active metabolite and shares some chemical features with 5HPP33 and lenalidomide in its addition of a hydroxyl or amine on the phthalimide ring.

The results of MM1s treatment with this panel of analogs is displayed in Figure 4A. Lenalidomide and pomalidomide showed IC50s of 35uM and 15uM, respectively, while both isomers of thalidomide and 5-OH-thalidomide showed almost no effect. (-)-Thalidomide, consistent with reports that it may be the active isomer, showed a very small anti-tumor effect (IC50 of ~500uM). Surprisingly, 5HPP33 showed remarkable anti-tumor activity.

Rationalizing an SAR from the biological effects observed in this small screen was difficult. The great increase in efficacy seen from the inclusion of an amino group on the phthalimide ring (in lenalidomide and pomalidomide) indicated that this region of the molecule was critical for activity, consistent with previous reports (Muller *et al.*, 1999). On the other hand, replacement of the glutaramide ring with a similar benzyl-di-tert-butyl ring (in 5HPP33) also markedly increased the activity. Addition of a hydroxyl group in the five position did not appreciably alter the IC50 of thalidomide, but the same position hydroxyl appears, according to literature reports, to be required for 5HPPP33 (Noguchi *et al.*, 2005). In sum, no consistent pattern emerges from the data which would suggest one particular region of the molecule is primarily responsible for its intracellular binding profile.

5HPP33 as a potential lead for drug development and Target ID

We were interested in the robust inhibition displayed by 5HPP33 in our initial cell line tests, so we tested the same panel of thalidomide analogs against CD34+ control (non-transformed) cells to determine which thalidomide derivatives, if any, displayed evidence *in vitro* for a therapeutic index (Figure 4B). Notably, none of the thalidomide analogs other than 5HPP33 and (-)-Thalidomide showed any greater inhibition of cells than DMSO control alone. The IC50 of 5HPP33 was 232nM in MM1s and 23.7uM in CD34 positive control cells, defining a therapeutic index of 102.1; by comparison Gleevec has an *in vitro* therapeutic index ranging from 57 to 243 depending on tested cell line (Topaly *et al.*, 2002). These results indicate that 5HPP33 may have unique anti-cancer properties in the thalidomide derivatives class and be

a lead for future drug development along these lines. It has been proposed as an inhibitor of tubulin polymerization (Iguchi *et al.*, 2008) but was initially reported for its anti-immunogenic properties (Miyachi *et al.*, 2007). Any other substituent of the benzyl ring on 5HPP33 smaller than a tert-butyl group fully disrupted its efficacy, suggesting this end of the molecule was critical for the effect of the drug.

Despite the potential of 5HPP33 for novel development, we felt that the background literature and clinical use of lenalidomide, which shows no inhibition of CD34+ cells, was the most suited to further investigation by fluoruous proteomics. We therefore chose to move ahead with lenalidomide as our primary drug of investigation.

Lenalidomide in a zebrafish model

Recent reports had relied on zebrafish models to identify the intracellular binders and effects of thalidomide by a proteomics experiment similar to the one we proposed to perform with lenalidomide. That same report included the observation of major morphogenic alterations during zebrafish development with thalidomide treatment (Ito *et al.*, 2010). We therefore wondered whether lenalidomide, which in rabbit models has less teratogenicity than thalidomide, would also show smaller teratogenic effects in zebrafish than thalidomide. We had already observed the widely divergent profiles of lenalidomide and thalidomide on myeloma cell treatment, and an extra phenotypic comparison would prove additionally useful for later analysis of proteomics results. Specifically, if CRBN is the intracellular target of thalidomide that is responsible for its teratogenicity, and lenalidomide is not, in fact, teratogenic, it naturally suggests the hypothesis that lenalidomide has a different target than thalidomide (and therefore CRBN might not be robustly observed in proteomics experiments). If, on the other hand, lenalidomide is teratogenic, it suggests that CRBN may be its primary intracellular target and should show up in any proteomics screen of lenalidomide.

We therefore replicated previous experiments by treating WT zebrafish with lenalidomide at concentrations ranging from 400 to 25 uM as previously reported. Briefly, zebrafish were dechorionated at 4hpf and treated with drug continuously for up to 72 hours, observed by light microscopy, and fixed for *in situ* and further microscopy. During this time, we did not observe any of the previously reported teratogenic effects of thalidomide on zebrafish embryos. Specifically, both pectoral fins and otic vessels developed normally, while reported changes with thalidomide were observed as previously reported. It is possible that lenalidomide, which is slightly more polar than thalidomide, was being hydrolyzed or otherwise broken down in media, thereby lowering the concentration below requisite levels. The required dose of thalidomide treatment had previously been determined empirically and most of the major effects only seen at higher doses, so there was some concern. To alleviate this concern, we monitored the lenalidomide in the media by LC-MS over the time course of treatment, and observed no significant drop in concentration (data not shown). We concluded that lenalidomide does not have the teratogenic effects of thalidomide in a zebrafish model. Interestingly, high doses of lenalidomide were also tested in rabbits and found not to be teratogenic there (Christian *et al.*, 2007). Given the new studies on lenalidomide mechanism cited in the introduction, it is a remarkable synthesis with our experiments that lenalidomide may have such divergent properties in this regard from lenalidomide.

Synthesis and testing of a lenalidomide-fluorous probe

With our data from both cell lines and zebrafish we therefore began the first steps towards a fluorous proteomics experiment involving lenalidomide by synthesizing a fluorous lenalidomide probe (Figure 3B). Synthetic methods and yields are discussed in Methods.

We chose to use the phthalimide amine on lenalidomide for our linker moiety for two reasons: ease of chemical access, and the evidence from 5HPP33 that steric effects on the glutaramide ring can effect major changes in the phenotypic profile of thalidomide derivatives. While differences have been

observed between hydroxyl and amino groups on the phthalimide (and their respective positions around the ring), this was not determined to be as critical of a concern.

Once in possession of a fluoruous lenalidomide (f-len) probe, we wondered whether the probe would show *in vitro* efficacy similar to lenalidomide. We therefore treated MM1s cells with f-len and lenalidomide (Figure 5). No inhibition was observed with f-len greater than DMSO control. We therefore wondered whether the fluoruous tag was preventing intracellular efficacy – which might be a major concern for proteomics experiments – or whether the probe was simply failing to penetrate cells at a sufficient concentration due to the highly unique fluoruous tag. We therefore treated cells for four days with lenalidomide, removed the media, lysed the treated cells, and looked for the presence of lenalidomide in both a cell and media fraction by LC-MS. After 4 days treatment with lenalidomide, both fractions showed significant presence of lenalidomide; after 4 days treatment with f-len, we did not observe any lenalidomide in the cell fraction though it was readily detectable in the media. We therefore concluded that f-len does not penetrate cells, and hoped that it might reliably recapitulate *in vitro* protein binding kinetics if used for proteomics experiments.

Establishing experimental conditions for fluoruous proteomics

With a fluoruous probe in hand, we wanted to be sure that we could perform a fluoruous separation of drug and resin from a complex mixture before attempting to use the probe for protein isolation. We therefore added probe to biological media and lysate and washed the resulting mixture over fluoruous resin. We then used LC-MS to identify any small molecules bound the fluoruous resin, and observed only fluoruous lenalidomide as the major binder. After elution and purification, we found that we could reliably recover 85% of the fluoruous probe from the complex mixture we tested. We concluded, therefore, that fluoruous pull-downs may work under typical proteomics conditions and might be relied upon to separate proteins from a complex mixture.

To further ensure that the fluoruous probe was robustly bound and would only elute under appropriate solvent conditions and not develop interference from a competing drug, we incubated another fluoruous tagged molecule (perphenazine) which was readily available to us with fluoruous resin with or without the presence of competing unbound perphenazine in the mixture. We then washed the resin, eluted under typical experimental conditions, and observed whether we could recover a significant percentage of our original probe with mass spectrometry. We were indeed able to recover nearly all of the originally bound probe, and it was not at all effected by the presence of competing drug, which was easily washed away and did not bind the fluoruous resin (Figure S1). This gave us further proof-of-principle that our fluoruous strategy was chemically specific and robust.

We then turned our attention to optimal protein lysis conditions for use with a fluoruous probe. Buffer conditions for the lysis and recovery of proteins have been investigated (Winkler *et al.*, 2009), but we sought to define for ourselves an approach which would maximize the yield of protein in native conformation from the largest possible subset of cellular organelles. Generally, the harsher the buffer conditions, the larger the percentage of the proteome which can be recovered; at the same time, such an approach necessarily denatures a large number of proteins, making them unsuitable for drug-affinity proteomics. The optimal lysis conditions would preserve native activity while generating good yield of protein.

We obtained Jurkat leukemia cells which had been engineered to express green fluorescent protein (GFP), which can readily be measured in cell lysates, as a rapid comparison method for the isolation of proteins with native activity. To quantify protein yield we performed a standard bicinchoninic acid assay.

We tested a variety of proprietary commercial lysis media as well as traditional lysis buffer supplemented by a variety of detergents. The results are displayed in Figure 6. Consistent with previous reports, we found that the addition of non-ionic detergents NP-40 and Pluronic F-127 to native lysis

buffer greatly increased yield extraction and yield activity as compared to native buffer alone. Since mixtures of detergents have sometimes been used to increase extraction efficiency (Iwata *et al.*, 2003), we also tested a variety of binary combinations of detergents. We found that the addition of the octyl-beta-glucosidase to Pluronic F-127 showed a further increase in extraction efficiency to as high as 1% SDS without any of the denaturing effect observed with such a harsh treatment. We then tested fluorour probe recovery in this media, as described above, and saw f-len probe recovery equal to that which was observed in cell media (~85%), indicating that this buffer system was suitable for fluorour proteomics.

Fluorour proteomics of lenalidomide

With a suitable probe and proteome extraction conditions in hand, we lysed MM1s cells and separated the mixture by fluorour drug-affinity proteomics as displayed schematically in Figure 1A. Briefly, we incubated fluorour lenalidomide probe with lysates in the presence of fluorour resin, washed out unbound proteins, eluted, purified, and digested bound peptides with trypsin. Peptides were then injected into a mass spectrometer, and spectra were analyzed by ProteinPilot software for identification. A typical spectrum generated from an entire LC-MS/MS run is displayed in Figure 7A. Figures 7B and 7C display typical statistical analysis of a single LC-MS/MS peptide identification run which was performed and analyzed after each sample to check for accuracy of peptide identification.

As expected, fluorour resin bound very few peptides in a non-specific manner. Only 31 non-specific peptides were bound to fluorour resin (data not shown), roughly the same as in a blank sample, and including peptides such as keratin and actin which were commonly confounding in all experiments and can be easily removed from consideration for biological significance. Streptavidin resins, by contrast, generated up to roughly 200 non-specific interactions, even when using a resin specifically designed to minimize non-specific adsorption (Alex Kentsis, private communication). The contrast between the high specificity of fluorour and promiscuity of streptavidin gave us hope that we would be

able to specifically identify a large number of lenalidomide-binding peptides without the interference common in traditional drug-affinity proteomics.

We therefor performed fluoruous affinity proteomics by incubating fluoruous lenalidomide with and without the presence of competitor, eluted, and identified peptides. Quantification was performed using spectral counts and unique peptide calls were made by ProteinPilot with a reported confidence value for spectral matching. The results, after filtering only for peptides specifically bound to the probe, are displayed in Table 1.

Notably, we did not find CRBN to be a binder of our probe. We anticipated that given the structural similarity between the drugs, even if CRBN was not the major binder of lenalidomide as it is for thalidomide, we would at least see some CRBN bound to the probe. In this way we hoped it would act as an internal positive control for our experiment. Since no other specific proteins have been identified as binding lenalidomide or thalidomide, we had no further way of internally validating the results. To confirm that CRBN was not in fact in our sample and rule out the possibility that its signal was obscured during LC-MS/MS by higher-ranking binders, we obtained antibodies for CRBN and tested affinity-purified lysates as well as native MM1s lysates for the presence of CRBN. In both cases we did not observe CRBN signal. The anti-CRBN antibodies are polyclonal and not well-validated, and we did not proceed further to validate them; nonetheless, it remains possible that CRBN was simply not part of the proteome of MM1s cells at sufficient levels to be detected by our experiments.

The list of identified peptides was submitted to DAVID for GO term analysis, and found to be overrepresented for proteins involved in nucleotide binding, mitochondrial space, and induction of apoptosis (all $p < .0001$). Notable genes included apoptosis inducing factor, chromodomain-helicase binding protein 7, and Gas1, which have been elsewhere associated with cancer or developmental diseases (Martinelli and Fan, 2007; Bajpai *et al.*, 2010).

Soon after we completed this experiment, it was reported the CRBN indeed bound lenalidomide in another group's work (Ebert lab, private communication). Without observing CRBN in our studies, we were unsure as to the validity of the rest of our identifications. Therefore, in order to continue testing fluoruous proteomics, we moved on to repeating the procedure with a second drug for Target ID, the BET bromodomain inhibitor JQ1.

JQ1 in T-ALL

The novel thieno-triazolo-1,4-diazepine JQ1 (Figure 8) binds selectively and with high affinity to the acetyllysine binding pocket of the conserved bromodomain and extra-terminal domain (BET) protein family, comprised of BRD2, BRD3, BRD4 and BRDT. BRD3 and BRD4 are translocated with the *NUT* gene in a rare form of squamous carcinoma (French *et al.*, 2008), and an RNAi screen identified BRD4 as a potential therapeutic target in acute myelogenous leukemia (Zuber *et al.*, 2011). Notably, inhibition of BRD4 is thought to selectively disrupt malignant cells by downregulating chromatin-mediated signal transduction at several loci, including *MYC*, which encodes the oncoprotein c-Myc.

JQ1 has been under investigation in several other cancer types and has recently shown potential in the treatment of T-ALL *in vitro*. Similar to our strategy with lenalidomide, we treated KOPTK1 cells (a T-ALL cell line) with JQ1 to establish its pharmacological profile (Figure 9). We found robust inhibition of KOPTK proliferation with an IC₅₀ of 130nM, two orders of magnitude higher than lenalidomide. We hoped the more specific binding of JQ1 would allow for a better proof-of-method for fluoruous drug affinity proteomics and the work on JQ1 in T-ALL elsewhere in the lab would find a good counterpoint in fluoruous proteomics data generated for JQ1.

Biotinylated JQ1 drug-affinity chromatography

We obtained fluoruous and biotinylated JQ1 probes for a direct method comparison between fluoruous and biotin-based identification (kindly provided by Jason Marrineau, Bradner Lab). The structure of the probes is displayed in Figure 8 (only fluoruous probe shown; biotin probe synthesis is discussed in a publication *in press* and not presented here).

We performed the previously reported drug-affinity/peptide identification protocol, first with biotinylated JQ1. The results of this pull down are displayed in Table 2. We observed a significant number of non-specifically bound peptides (157), consistent with expectations for a streptavidin matrix. Nonetheless, once filtering out for non-specific interactions, we were able to identify the known binders of JQ1 (BRD2, BRD3, BRD4) as well as many other potential binders of equal significance. HSPA1A, HSPA8 and TUBB have all been associated with cancer; GO term analysis revealed significant overrepresentation of proteins annotated for involvement in acetylation, translation, MHC class 1 binding and microtubule polymerization ($p < 1e-26$). Notably several ribosomal proteins associated with Diamond-Blackfan anemia (RPL11, 17, 19 and 7) were also identified, as well as pyruvate kinase M2, which has been widely reported in recent literature as critical to the pathogenesis of many cancers (Vander Heiden *et al.*, 2009). Several heat shock proteins on the list have also been identified as playing a role in various diseases.

Fluoruous proteomics of JQ1.

Encouraged by the observation of positive internal controls as well as potential novel binders of JQ1 using the biotinylated probe, we performed fluoruous drug-affinity chromatography on f-JQ1. Using SILAC-labeled cells, we quantified and identified specific binders to fluoruous-JQ1 following the previously described methods and generated a list of bound peptides (Table 3).

Surprisingly, while we found many specific binders of fluoruous JQ1, we could not identify a similar list of bound proteins to biotinylated JQ1 (which we had high confidence in as it included many of the known binders). A huge list of peptides was identified, only the top 100 of which were included in Table 3. BRD2, BRD3, and BRD4, the known binders of JQ1 which were visible in the biotinylated JQ affinity-chromatography, were not seen with fluoruous JQ1. Still, the list that was obtained had a number of binders in common with the JQ1 biotin list, including pyruvate kinase, though this may be a result of fair abundance of pyruvate kinase in cellular extracts. Notably the SET gene, which has been previously implicated in myeloid malignancies, was also identified (Nagata *et al.*, 1995). Functional annotation showed overrepresentation of genes involved in acetylation and methylation ($p < 1e-20$), raising the confidence that the list contains genes related to JQ1 activity.

Discussion

Summary

In this work, we attempted to apply a novel technique, which we termed fluoruous-affinity protetomics, to the traditional problem of drug-affinity chromatography for target ID. We chose two drugs, thalidomide and JQ1, as proof-of-concept systems with which to work. We established the pharmacokinetic profile of each in the cell lines of interest, determined for thalidomide which drug to test from a group of analogs, and designed probes based on our best-guess SAR for thalidomide.

We then established the conditions for fluoruous proteomics and tested the applicability of the fluoruous technique at several intermediate steps. At the same time we investigated the biology of lenalidomide and JQ1, identifying in the case of the former a novel analog 5HPP33 which shows therapeutic potential, and establishing the applicability of JQ1 to treatment of T-ALL.

We investigated both lenalidomide and JQ1 by fluoruous proteomics with biotinylated JQ1 as a control. In each case, we identified a list of specifically bound peptides, but we did not consistently observe the known (or putatively known) binders in our samples (CRBN and the BRD family). As we were unsure of the value of our results, we chose to continue refining and repeating our screen technique rather than validating potential novel binders, except in the case of Biotin JQ1, where we observed proteins we were sure bound to JQ1, making this our highest-confidence list of identified peptides. Nonetheless, we identified a robust list of interesting proteins by fluoruous proteomics, some of which had known association with disease.

The mechanism of lenalidomide

When we initially set out on our experiments above, we attempted to both (1) develop a novel technology for target ID and (2) leverage that technology toward solving an important biological and chemical problem, the mechanism of action of lenalidomide. As noted in the introduction, several recent papers have had a major bearing on this second aim by in fact offering a solution to this problem. One of these papers also solved the crystal structure of lenalidomide in complex with CRBN and DDB-1 (Chamberlain *et al.*, 2014). In this paper, Chamberlain and colleagues note that lenalidomide is accommodated to CRBN in a tri-tryptophan hydrophobic pocket, with the glutaramide ring of lenalidomide sliding into this pocket and the pthalidimide (isoindolinone) group (which is differentially modified in lenalidomide and pomalidomide versus thalidomide) is exposed at the surface of the protein. The authors of this paper note that this binding pocket is highly conserved in orthologs of cereblon, implying that perhaps an as-yet unidentified natural ligand may occupy this space as an “adaptor-like” molecule for facilitating specific ubiquitination. It is intriguing, given these results, that 5HPP33, which replaces the glutaramide with the highly nonpolar but similarly-sized di-tert-butyl-benzyl group, is a very effective inhibitor of myeloma cell growth in our experiments (Figure 3A and 4A). The benzyl could very effectively hit this same pocket. An outstanding question – and one with great potential implications for drug design – is whether lenalidomide and its derivatives present a neomorphic structure for selective ubiquitination that is not a normal function of the protein. Evidence from other papers (Ito *et al.*, 2010) *implies*, but does not prove, that thalidomide works through creating a hypermorph (i.e., RNAi experiments knocking-down CRBN recapitulate the thalidomide phenotype seen in chicks and zebrafish). Given that lenalidomide and thalidomide, as shown here and previously, have some vastly different phenotypes (differences in teratogenicity in zebrafish shown here; rabbits as noted previously; differential induction of IL-2 in recent work), it is tempting to speculate that minor alterations to this molecule could enable intriguing new properties and indirectly druggable “targets.”

Control of ubiquitination may be a new frontier in drug design, and evidence presented here in lenalidomide derivatives both extends, supports, and offers intriguing new possibilities for this line of work.

Difficulties (and possible successes) with fluoruous proteomics

The greatest disappointment in our work was the variable quality of outcome of peptide ID. In several experiments, we observed a robust list of interesting proteins bound to our probe. Nonetheless we failed to observe, in the case of both fluoruous probes, the expected internal positive controls – peptides known to bind to our probe as high hits on our screen.

It is possible that we were simply “unlucky” in our probe design. Lenalidomide is an extremely complex molecule, and a simple SAR is almost impossible to derive from the literature (see Table S1) or from our own experiments; from the recent experiments, it seems as if putting our linker on the phthalimide was “correct” from a structural ligand-protein relationship view, but it is impossible to know how the size of the linker would affect the binding of the glutaramide to the putative tri-tryptophan pocket discussed just above.

Our probe was designed chiefly for ease of chemical synthesis, but any piece of the probe – the amide coupling, the linker length, its placement on the phthalimide amine, using amide rather than another form of coupling to linker – could conceivably alter the chemistry of lenalidomide so that it did not bind its normal *in vivo* targets in our experiments. In any event, it shows the sensitivity of proteomics experiments to all downstream aspects of the experimental set up, and the great biological diversity that might be revealed (sometimes unintentionally) when pursuing these experiments. Such diversity can, as in this case, be a confounder that makes troubleshooting as difficult as the diversity itself might be illuminating.

The comparison between biotinylated JQ1 and fluoruous JQ1 was likewise by equal measures disappointing and intriguing. With a biotin probe we observed all three of the known binders to JQ1 in

KOPTK cells (BRD2, BRD3, and BRD4), in addition to a long list of even more tightly bound peptides which may be of continuing interest to the JQ1 field going forward. Several have association with disease, cancer, translation and acetylation; some are likely members of the histone reader complex (and thereby co-purified with the BRD proteins) that have not yet been fully identified in other experiments. Of particular note here was the high spot of pyruvate kinase M2 on this list.

On the other hand, fluoruous proteomics in the same cell system and under the same conditions did not show any of the BRD proteins, though it did share a number of other identifications in common with the biotin probe. Why would the fluoruous and biotin lists diverge so completely? It is possible that the fluoruous resin, while minimizing non-specific interactions, loses some measure of stabilizing effect on peptides that is present with a streptavidin resin; and that while tag-matrix interactions may be stronger in the fluoruous case (and protein-matrix interactions weaker), somehow the protein was washed away during our experimental set up due to this weak binding. Without further experiments, especially additional SILAC or tag-based quantitation, it is difficult to say more about the possible failings of fluoruous proteomics. The major future directions that could develop out of this work are (1) a further investigation of fluoruous proteomics, including troubleshooting; and (2), a validation of any novel targets observed in the experiments contained here.

We were encouraged by the prospects of fluoruous proteomics. But future, more controlled experiments might be required for validation of the technique itself, in which the balance of problems chosen shifts slightly from “known and unknown biology” (which we chose, to maximize both biological interest and method validation) closer to the realm of “fully known biology.” Fluoruous proteomics may still hold great potential for target ID, but we would proceed with caution.

Acknowledgments

I would like to thank Alex Kentsis of the Look Lab, who supervised most of the work and was a constant source of guidance, help and compassion. Jason Marrineau, of the Bradner Lab, also greatly contributed to this work and supervised the many stumbling hours of my first official foray into organic synthesis. Thomas Look and the rest of the members of the Look Lab provided stimulating discussion and interesting place to work; Jun Qi, Chris Ott, and Joanna Yi of the Bradner Lab helped me with various aspects of the project, provided cells and drugs (of the testable-in-cell-culture kind), and showed me how to use a dry-transfer western blot machine, which saved at least one weekend of my summer. Finally, my advisor, Jay Bradner, provided constant guidance, help, and encouragement.

Figures and Tables

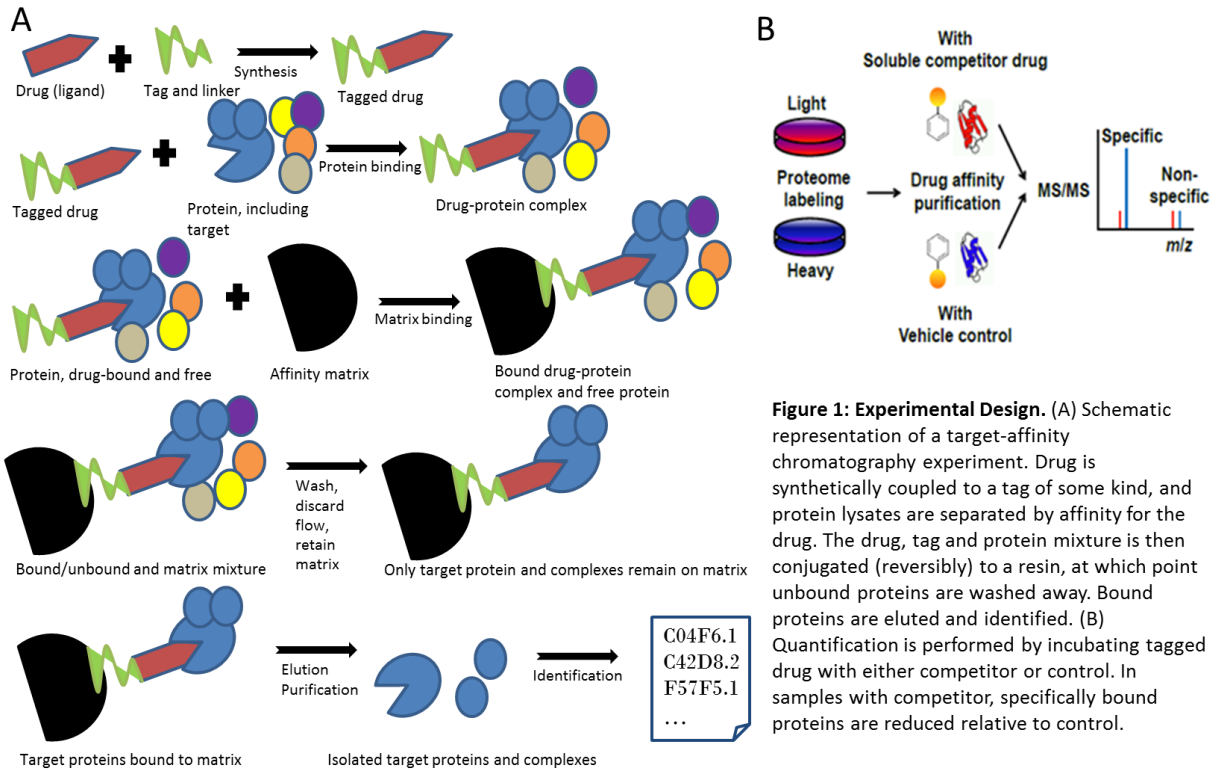


Figure 1: Experimental Design. (A) Schematic representation of a target-affinity chromatography experiment. Drug is synthetically coupled to a tag of some kind, and protein lysates are separated by affinity for the drug. The drug, tag and protein mixture is then conjugated (reversibly) to a resin, at which point unbound proteins are washed away. Bound proteins are eluted and identified. (B) Quantification is performed by incubating tagged drug with either competitor or control. In samples with competitor, specifically bound proteins are reduced relative to control.

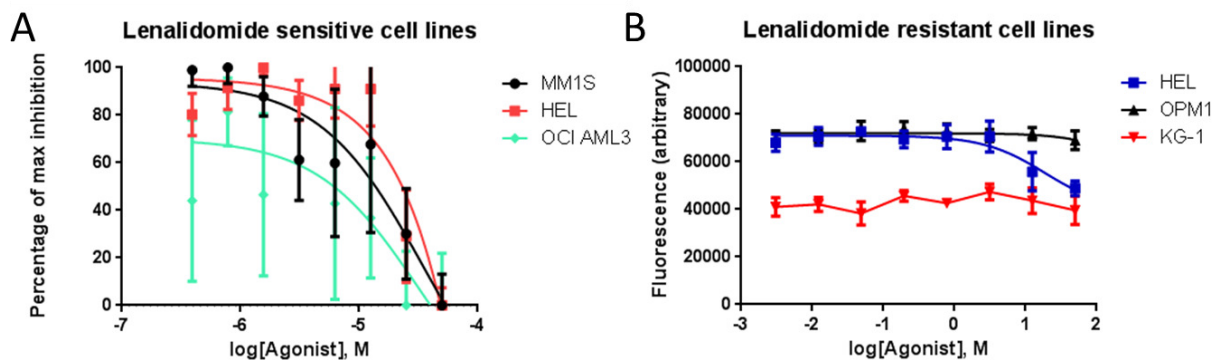


Figure 2: Distinct lenalidomide treatment profiles. We treated a panel of cell lines with lenalidomide to determine the kinetics and IC50 of lenalidomide treatment. (A) Sensitive cell lines showed a long, sloping inhibition profile, rather than a sharp one, and high concentrations were no more potent than DMSO (not shown). (B) Several cell lines were lenalidomide resistant and showed minimal or no response to lenalidomide even at higher doses than in (A).

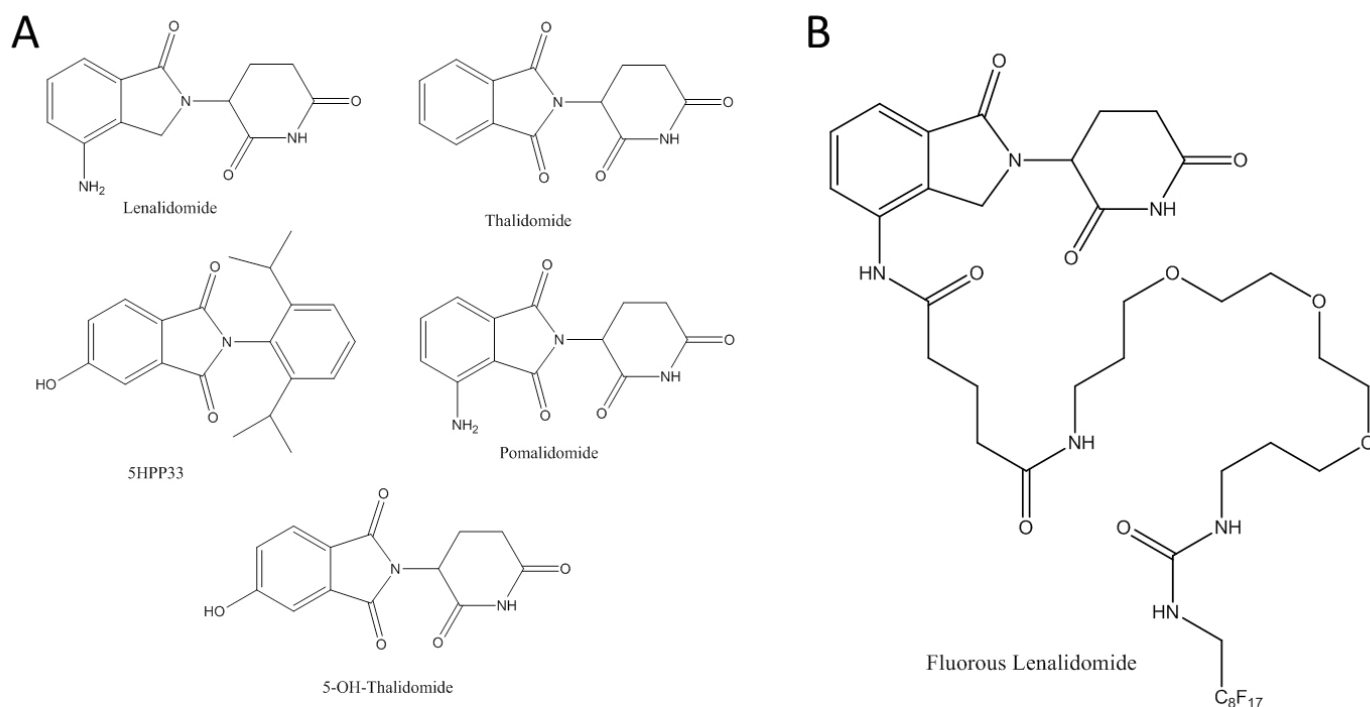


Figure 3: Chemical structure of thalidomide derivatives. (A) The chemical structure of thalidomide and its derivatives. Thalidomide is divided into a phthalimide group (left side of molecule) and glutaramide group (right side). Lenalidomide, pomalidomide, 5HPP33 and 5-OH-Thalidomide have a hydroxyl or amino group on the phthalimide. 5HPP33 replaces the glutaramide with a di-t-butyl benzyl group. (B) The structure of the synthesized fluorous lenalidomide probe. The amine of lenalidomide was coupled to a long PEG linker and via urea to a fluorine tag.

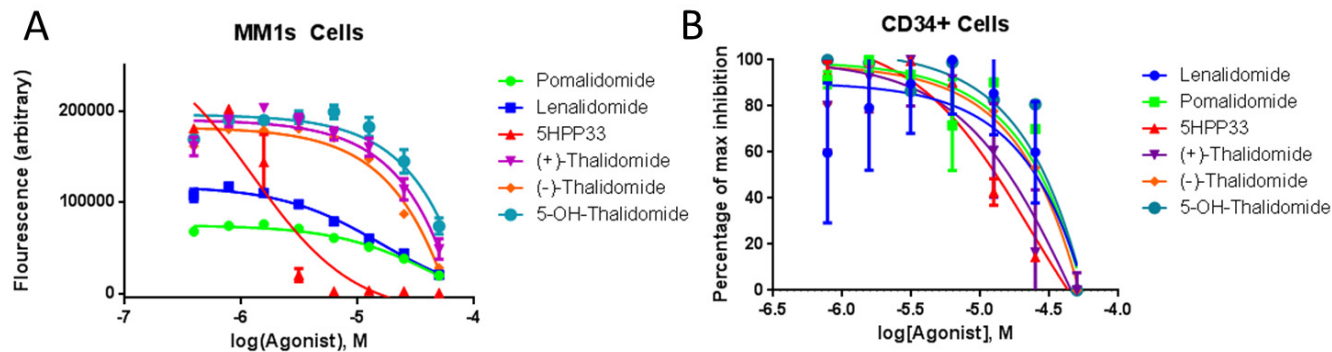


Figure 4: Thalidomide derivatives. We tested a panel of thalidomide derivatives against transformed (A) and control (B) cell lines.

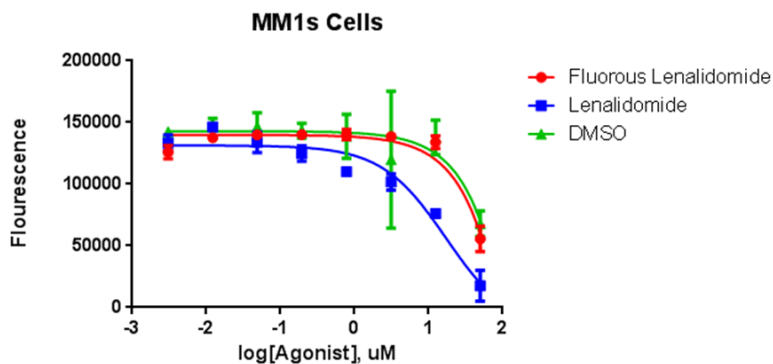


Figure 5: Fluorous lenalidomide does not inhibit cell growth. We tested fluoruous lenalidomide for ability to inhibit cell growth and for penetration of cell membranes. F-len did not display inhibition in growth assays and did not appear to penetrate cells (see text).

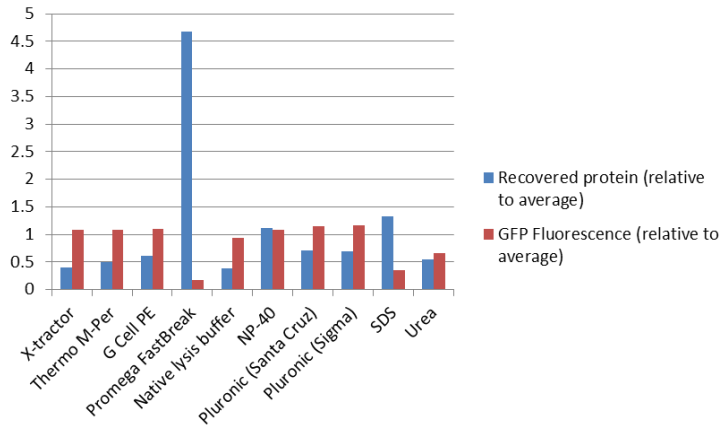


Figure 6: Protein lysis conditions. There is a trade-off between proteome yield and maintenance of native activity. To find the best balance, we tested a variety of proprietary buffers (left four) as well as native lysis buffer supplemented with various detergents (right six). We measured recovered protein in two cell lines and GFP fluorescence from a GFP-expressing cell line as a proxy for native conformation retention. Average values are displayed.

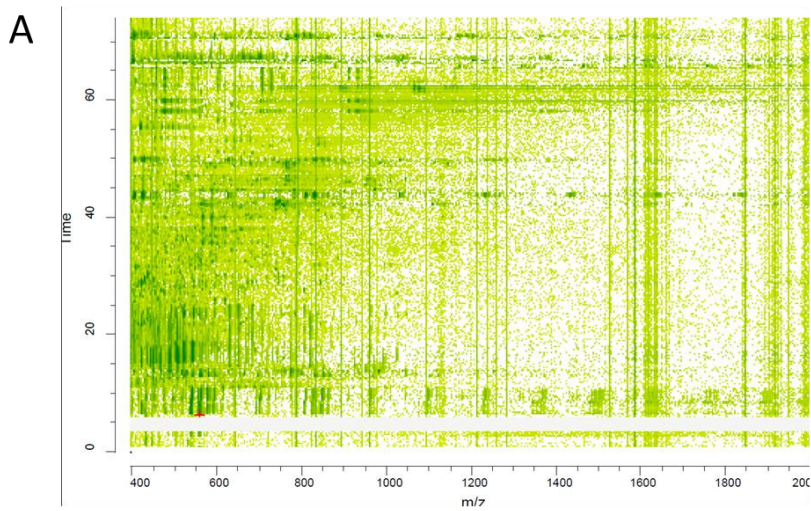
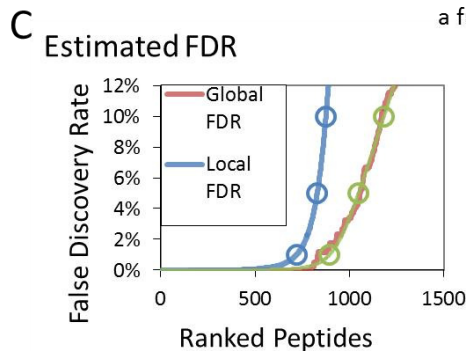
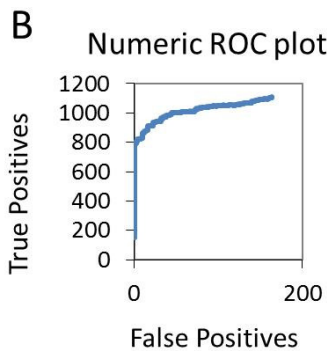


Figure 7: Representative LC-MS/MS based identification. Peptides from drug-affinity chromatography were identified using LC-MS/MS identification and quantification. (A) Representative m/z spectrum (x axis) versus elution time (y axis). Green indicates relative peak intensity. (B) Representative ROC for peptide identification, indicating high confidence in a large number of peptides before false positives are identified, allowing for easy delimiting of high-confidence peptides. (C) Identified peptides as a function of false discovery rate.



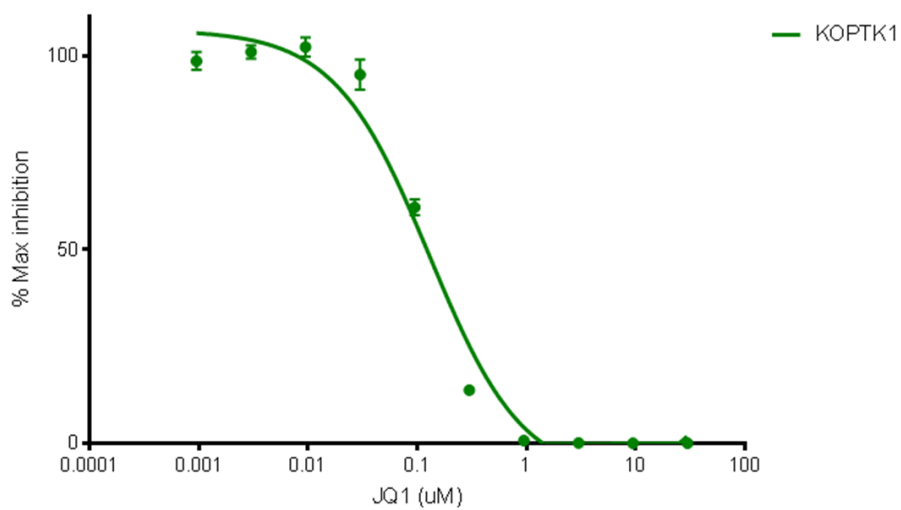
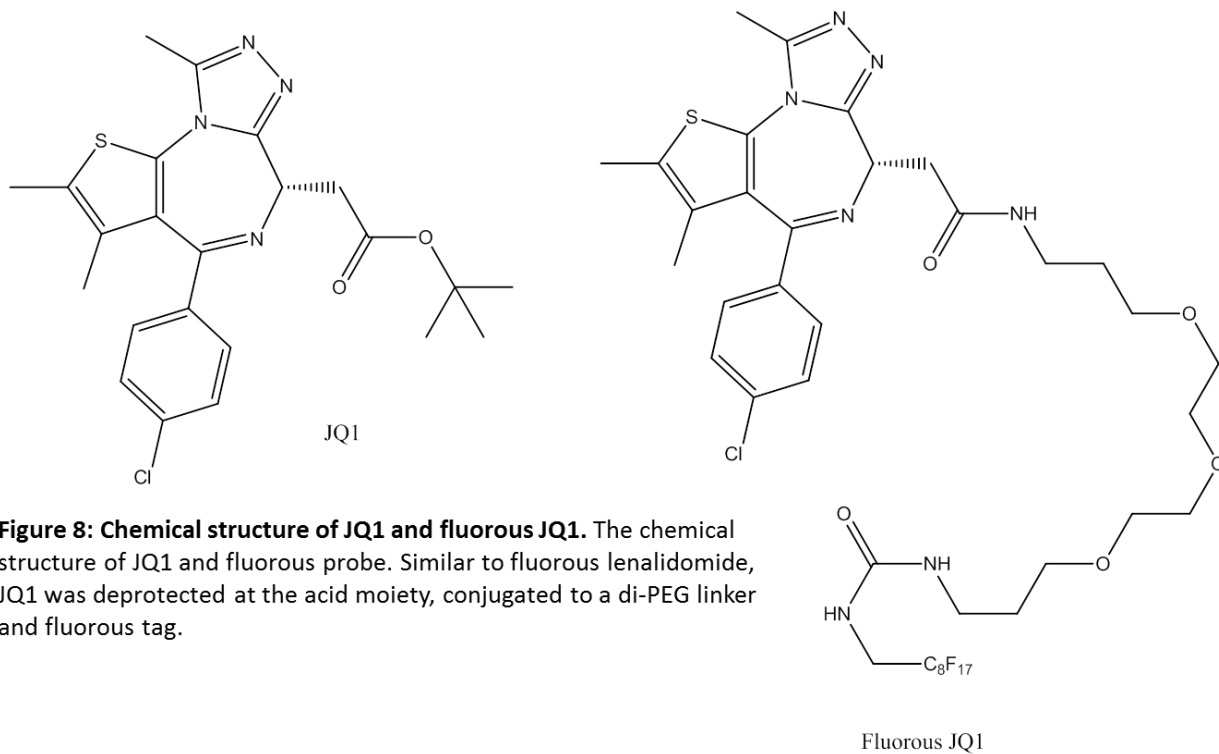


Figure 9: JQ1 inhibition of a T-ALL cell line. We treated KOPTK1, a T-ALL cell line, with JQ1, with a fit IC50 of 130nM.

Table 1: Peptides identified by lenalidomide fluoruous proteomics

Peptide ID	Confidence
40S ribosomal protein S3 OS=Homo sapiens GN=RPS3 PE=1 SV=2	99
Dolichyl-diphosphooligosaccharide--protein glycosyltransferase subunit DAD1 OS=Homo sapiens GN=DAD1 PE=1 SV=3	99
Cystatin-A OS=Homo sapiens GN=CSTA PE=1 SV=1	99
Uncharacterized protein C8orf86 OS=Homo sapiens GN=C8orf86 PE=2 SV=1	99
40S ribosomal protein S19 OS=Homo sapiens GN=RPS19 PE=1 SV=2	97.67
E3 ubiquitin-protein ligase BRE1A OS=Homo sapiens GN=RNF20 PE=1 SV=2	94.49
Macoilin OS=Homo sapiens GN=TMEM57 PE=1 SV=1	98.51
Zyxin OS=Homo sapiens GN=ZYG1 PE=1 SV=1	91.73
Tricarboxylate transport protein, mitochondrial OS=Homo sapiens GN=SLC25A1 PE=1 SV=2	83.29
Adenylate cyclase type 2 OS=Homo sapiens GN=ADCY2 PE=1 SV=5	82.18
Chromodomain-helicase-DNA-binding protein 7 OS=Homo sapiens GN=CHD7 PE=1 SV=3	80.62
Serine protease HTRA2, mitochondrial OS=Homo sapiens GN=HTRA2 PE=1 SV=2; Isoform 3 of Serine protease HTRA2, mitochondrial OS=Homo sapiens GN=HTRA2; Isoform 2 of Serine protease HTRA2, mitochondrial OS=Homo sapiens GN=HTRA2	80.39
Huntingtin-interacting protein 1-related protein OS=Homo sapiens GN=HIP1R PE=1 SV=2	78.23
Ganglioside-induced differentiation-associated protein 2 OS=Homo sapiens GN=GDAP2 PE=2 SV=1; Isoform 2 of Ganglioside-induced differentiation-associated protein 2 OS=Homo sapiens GN=GDAP2	75.64
1-phosphatidylinositol-4,5-bisphosphate phosphodiesterase delta-1 OS=Homo sapiens GN=PLCD1 PE=1 SV=2	73.42
Heterogeneous nuclear ribonucleoprotein L OS=Homo sapiens GN=HNRNPL PE=1 SV=2	74.09
[Pyruvate dehydrogenase [acetyl-transferring]]-phosphatase 2, mitochondrial OS=Homo sapiens GN=PDP2 PE=2 SV=2	70.85
Isoform 4 of Diphthine synthase OS=Homo sapiens GN=DPH5	71.29
Ankyrin repeat and LEM domain-containing protein 2 OS=Homo sapiens GN=ANKLE2 PE=1 SV=4	69.27
Armadillo repeat-containing X-linked protein 3 OS=Homo sapiens GN=ARMCX3 PE=1 SV=1	66.26
Motor neuron and pancreas homeobox protein 1 OS=Homo sapiens GN=MNX1 PE=1 SV=3	58.9
ATPase family AAA domain-containing protein 5 OS=Homo sapiens GN=ATAD5 PE=1 SV=4	61.52
Growth arrest-specific protein 1 OS=Homo sapiens GN=GAS1 PE=1 SV=2	62.79
Guanylate cyclase soluble subunit beta-1 OS=Homo sapiens GN=GUCY1B3 PE=1 SV=1; Isoform HSGC-2 of Guanylate cyclase soluble subunit beta-1 OS=Homo sapiens GN=GUCY1B3	60.89
Brain-enriched guanylate kinase-associated protein OS=Homo sapiens GN=BEGAIN PE=1 SV=1	59.81
Schlafen family member 5 OS=Homo sapiens GN=SLFN5 PE=1 SV=1	56.44
26S proteasome non-ATPase regulatory subunit 1 OS=Homo sapiens GN=PSMD1 PE=1 SV=2; Isoform 2 of 26S proteasome non-ATPase regulatory subunit 1 OS=Homo sapiens GN=PSMD1	53.74
Heterogeneous nuclear ribonucleoprotein M OS=Homo sapiens GN=HNRNPM PE=1 SV=3; Isoform 2 of Heterogeneous nuclear ribonucleoprotein M OS=Homo sapiens GN=HNRNPM	80.49
Apoptosis-inducing factor 1, mitochondrial OS=Homo sapiens GN=AIFM1 PE=1 SV=1	48.63
Leucyl-cystinyl aminopeptidase OS=Homo sapiens GN=LNPEP PE=1 SV=3; Isoform 3 of Leucyl-cystinyl aminopeptidase OS=Homo sapiens GN=LNPEP; Isoform 2 of Leucyl-cystinyl aminopeptidase OS=Homo sapiens GN=LNPEP	49.66

Table 2: Selected peptides bound to biotin-JQ1

Peptide ID	Spectral count
ATP5B ATP synthase subunit beta, mitochondrial	23
RPS19 40S ribosomal protein S19	22
SLK Isoform 2 of STE20-like serine/threonine-protein kinase	19
SUB1 Activated RNA polymerase II transcriptional coactivator p15	19
DDX5 Probable ATP-dependent RNA helicase DDX5	17
RPS3 40S ribosomal protein S3	17
HSPD1 60 kDa heat shock protein, mitochondrial	16
NACA nascent polypeptide-associated complex alpha subunit isoform a	16
EEF1A1;EEF1AL3 Putative elongation factor 1-alpha-like 3	15
TUBB Tubulin beta chain	15
TUBB2C Tubulin beta-2C chain	15
HSPA8 Isoform 1 of Heat shock cognate 71 kDa protein	14
RPS7 40S ribosomal protein S7	14
RPS4X 40S ribosomal protein S4, X isoform	12
PRDX1 19 kDa protein	10
SRP14 Signal recognition particle 14 kDa protein	10
HSPA5 HSPA5 protein	9
CASP12 31 kDa protein	8
HSP90AB1 Heat shock protein HSP 90-beta	8
PKM2 Isoform M2 of Pyruvate kinase isozymes M1/M2	8
RPS17 40S ribosomal protein S17	8
ATP5A1 ATP synthase subunit alpha, mitochondrial	7
RPL9 60S ribosomal protein L9	7
RPL11 Isoform 1 of 60S ribosomal protein L11	6
RPL30 Putative uncharacterized protein RPL30 (Fragment)	6
RPS10 40S ribosomal protein S10	6
TUBA1B cDNA FLJ60097, highly similar to Tubulin alpha-ubiquitous chain	6
BRD3 Isoform 1 of Bromodomain-containing protein 3	5
C11orf31 Selenoprotein H	5
RPS14 40S ribosomal protein S14	5
RPS20 ribosomal protein S20 isoform 1	5
CEP170 Isoform 2 of Centrosomal protein of 170 kDa	4
HIST1H1D Histone H1.3	4
MAP4 110 kDa protein	4
MRPL14 39S ribosomal protein L14, mitochondrial	4
RPL23 60S ribosomal protein L23	4
RPL38 60S ribosomal protein L38	4
THOC4 THO complex 4	4
BRD4 80 kDa protein	3
HMCN1 Hemicentin 1	3
HSPA1A;HSPA1B Heat shock 70 kDa protein 1A/1B	3
MAP7 Isoform 1 of Ensconsin	3
NSUN5 Isoform 2 of Putative methyltransferase NSUN5	3
RPL22 60S ribosomal protein L22	3
RPL35 60S ribosomal protein L35	3
RPS15A 40S ribosomal protein S15a	3
RPS5 40S ribosomal protein S5	3
ANXA2 Isoform 1 of Annexin A2	2
BRD2 Isoform 1 of Bromodomain-containing protein 2	2
DCAF13 WD repeats and SOF1 domain containing	2
HSPA9 cDNA FLJ51903, highly similar to Stress-70 protein, mitochondrial	2
NUSAP1 Isoform 2 of Nucleolar and spindle-associated protein 1	2
PPIA Peptidyl-prolyl cis-trans isomerase A	2
RPS9 40S ribosomal protein S9	2
SNRNP3 cDNA FLJ51872, highly similar to Small nuclear ribonucleoprotein Sm D	2
STK10 Serine/threonine-protein kinase 10	1

Table 3: Top 100 peptides bound to f-JQ1

Name	Description	Spectral Count
ENOA	Alpha-enolase OS=Homo sapiens GN=ENO1 PE=1 SV=2	23
G3P	Glyceraldehyde-3-phosphate dehydrogenase OS=Homo sapiens GN=GAPDH PE=1 SV=3	16
TBB5	Tubulin beta chain OS=Homo sapiens GN=TUBB PE=1 SV=2	14
TPIS	Triosephosphate isomerase OS=Homo sapiens GN=TP11 PE=1 SV=3	13
TPIS	Isoform 2 of Triosephosphate isomerase OS=Homo sapiens GN=TP11	13
K2C5	Keratin, type II cytoskeletal 5 OS=Homo sapiens GN=KRT5 PE=1 SV=3	11
TBA1B	Tubulin alpha-1B chain OS=Homo sapiens GN=TUBA1B PE=1 SV=1	10
PGK1	Phosphoglycerate kinase 1 OS=Homo sapiens GN=PGK1 PE=1 SV=3	9
FUBP2	Isoform 2 of Far upstream element-binding protein 2 OS=Homo sapiens GN=KHSRP	9
FUBP2	Far upstream element-binding protein 2 OS=Homo sapiens GN=KHSRP PE=1 SV=4	9
HS90B	Heat shock protein HSP 90-beta OS=Homo sapiens GN=HSP90AB1 PE=1 SV=4	8
KPYM	Pyruvate kinase isozymes M1/M2 OS=Homo sapiens GN=PKM2 PE=1 SV=4	8
LDHA	L-lactate dehydrogenase A chain OS=Homo sapiens GN=LDHA PE=1 SV=2	8
LDHA	Isoform 2 of L-lactate dehydrogenase A chain OS=Homo sapiens GN=LDHA	8
1433Z	14-3-3 protein zeta/delta OS=Homo sapiens GN=YWHAZ PE=1 SV=1	8
LDHB	L-lactate dehydrogenase B chain OS=Homo sapiens GN=LDHB PE=1 SV=2	8
ATPA	ATP synthase subunit alpha, mitochondrial OS=Homo sapiens GN=ATP5A1 PE=1 SV=1	7
HSP7C	Heat shock cognate 71 kDa protein OS=Homo sapiens GN=HSPA8 PE=1 SV=1	7
HSP7C	Isoform 2 of Heat shock cognate 71 kDa protein OS=Homo sapiens GN=HSPA8	7
CH60	60 kDa heat shock protein, mitochondrial OS=Homo sapiens GN=HSPD1 PE=1 SV=2	7
HS90A	Isoform 2 of Heat shock protein HSP 90-alpha OS=Homo sapiens GN=HSP90AA1	7
HS90A	Heat shock protein HSP 90-alpha OS=Homo sapiens GN=HSP90AA1 PE=1 SV=5	7
ATPB	ATP synthase subunit beta, mitochondrial OS=Homo sapiens GN=ATP5B PE=1 SV=3	6
PPIA	Peptidyl-prolyl cis-trans isomerase A OS=Homo sapiens GN=PPIA PE=1 SV=2	6
ACTBL	Beta-actin-like protein 2 OS=Homo sapiens GN=ACTBL2 PE=1 SV=2	6
COF1	Cofilin-1 OS=Homo sapiens GN=CFL1 PE=1 SV=3	5
MDHM	Malate dehydrogenase, mitochondrial OS=Homo sapiens GN=MDH2 PE=1 SV=3	5
EF1A3	Putative elongation factor 1-alpha-like 3 OS=Homo sapiens GN=EEF1A1P5 PE=5 SV=1	5
EF1A1	Elongation factor 1-alpha 1 OS=Homo sapiens GN=EF1A1 PE=1 SV=1	5
RLA2	60S acidic ribosomal protein P2 OS=Homo sapiens GN=RPLP2 PE=1 SV=1	4
VIME	Vimentin OS=Homo sapiens GN=VIM PE=1 SV=4	4
PLSL	Plastin-2 OS=Homo sapiens GN=LCP1 PE=1 SV=6	4
EF2	Elongation factor 2 OS=Homo sapiens GN=EEF2 PE=1 SV=4	4
1433B	14-3-3 protein beta/alpha OS=Homo sapiens GN=YWHAB PE=1 SV=3	4
1433B	Isoform Short of 14-3-3 protein beta/alpha OS=Homo sapiens GN=YWHAB	4
MOES	Moesin OS=Homo sapiens GN=MSN PE=1 SV=3	4
ROA1	Heterogeneous nuclear ribonucleoprotein A1 OS=Homo sapiens GN=HNRNPA1 PE=1 SV=5	4
ROA1	Isoform 2 of Heterogeneous nuclear ribonucleoprotein A1 OS=Homo sapiens GN=HNRNPA1	4
ROA1	Isoform A1-A of Heterogeneous nuclear ribonucleoprotein A1 OS=Homo sapiens GN=HNRNPA1	4
TIM44	Mitochondrial import inner membrane translocase subunit TIM44 OS=Homo sapiens GN=TIMM44 PE=1 SV=2	4
1433T	14-3-3 protein theta OS=Homo sapiens GN=YWHAQ PE=1 SV=1	4
RAN	GTP-binding nuclear protein Ran OS=Homo sapiens GN=RAN PE=1 SV=3	4
MIF	Macrophage migration inhibitory factor OS=Homo sapiens GN=MIF PE=1 SV=4	4
ROA2	Heterogeneous nuclear ribonucleoproteins A2/B1 OS=Homo sapiens GN=HNRNPA2B1 PE=1 SV=2	3
ROA2	Isoform A2 of Heterogeneous nuclear ribonucleoproteins A2/B1 OS=Homo sapiens GN=HNRNPA2B1	3
HNRPK	Heterogeneous nuclear ribonucleoprotein K OS=Homo sapiens GN=HNRNPK PE=1 SV=1	3
HNRPK	Isoform 3 of Heterogeneous nuclear ribonucleoprotein K OS=Homo sapiens GN=HNRNPK	3
HNRPK	Isoform 2 of Heterogeneous nuclear ribonucleoprotein K OS=Homo sapiens GN=HNRNPK	3
PROF1	Profilin-1 OS=Homo sapiens GN=PFN1 PE=1 SV=2	3
SET	Protein SET OS=Homo sapiens GN=SET PE=1 SV=3	3
SET	Isoform 2 of Protein SET OS=Homo sapiens GN=SET	3
ALDOA	Fructose-bisphosphate aldolase A OS=Homo sapiens GN=ALDOA PE=1 SV=2	3
TKT	Transketolase OS=Homo sapiens GN=TKT PE=1 SV=3	3
TPM3	Isoform 2 of Tropomyosin alpha-3 chain OS=Homo sapiens GN=TPM3	3
TPM3	Isoform 3 of Tropomyosin alpha-3 chain OS=Homo sapiens GN=TPM3	3
RL40	Ubiquitin-60S ribosomal protein L40 OS=Homo sapiens GN=UBA52 PE=1 SV=2	3
RS27A	Ubiquitin-40S ribosomal protein S27a OS=Homo sapiens GN=RPS27A PE=1 SV=2	3
UBC	Polyubiquitin-C OS=Homo sapiens GN=UBC PE=1 SV=2	3
UBB	Polyubiquitin-B OS=Homo sapiens GN=UBB PE=1 SV=1	3
CATA	Catalase OS=Homo sapiens GN=CAT PE=1 SV=3	3
TAGL2	Transgelin-2 OS=Homo sapiens GN=TAGLN2 PE=1 SV=3	3
PRDX1	Peroxisiredoxin-1 OS=Homo sapiens GN=PRDX1 PE=1 SV=1	3
STMN1	Stathmin OS=Homo sapiens GN=STMN1 PE=1 SV=3	3
STMN1	Isoform 2 of Stathmin OS=Homo sapiens GN=STMN1	3
SRSF3	Serine/arginine-rich splicing factor 3 OS=Homo sapiens GN=SRSF3 PE=1 SV=1	3
1433E	14-3-3 protein epsilon OS=Homo sapiens GN=YWHA E PE=1 SV=1	3
1433E	Isoform SV of 14-3-3 protein epsilon OS=Homo sapiens GN=YWHA E	3
HNRPD	Heterogeneous nuclear ribonucleoprotein D0 OS=Homo sapiens GN=HNRNPD PE=1 SV=1	2
G6PI	Glucose-6-phosphate isomerase OS=Homo sapiens GN=GPI PE=1 SV=4	2
HMG1	High mobility group protein B1 OS=Homo sapiens GN=HMG1 PE=1 SV=3	2
AN32A	Acidic leucine-rich nuclear phosphoprotein 32 family member A OS=Homo sapiens GN=ANP32A PE=1 SV=1	2
BAF	Barrier-to-autointegration factor OS=Homo sapiens GN=BANF1 PE=1 SV=1	2
PSME2	Proteasome activator complex subunit 2 OS=Homo sapiens GN=PSME2 PE=1 SV=4	2
H4	Histone H4 OS=Homo sapiens GN=HIST1H4A PE=1 SV=2	2
SMD3	Small nuclear ribonucleoprotein Sm D3 OS=Homo sapiens GN=SNRPD3 PE=1 SV=1	2
SH3L1	SH3 domain-binding glutamic acid-rich-like protein OS=Homo sapiens GN=SH3BGLR PE=1 SV=1	2
SODM	Superoxide dismutase [Mn], mitochondrial OS=Homo sapiens GN=SOD2 PE=1 SV=2	2
DCD	Dermcidin OS=Homo sapiens GN=DCD PE=1 SV=2	2
PA2G4	Proliferation-associated protein 2G4 OS=Homo sapiens GN=PA2G4 PE=1 SV=3	2
PEBP1	Phosphatidylethanolamine-binding protein 1 OS=Homo sapiens GN=PEBP1 PE=1 SV=3	2
CH10	10 kDa heat shock protein, mitochondrial OS=Homo sapiens GN=HSPE1 PE=1 SV=2	2
RL4	60S ribosomal protein L4 OS=Homo sapiens GN=RPL4 PE=1 SV=5	2
NUCL	Nucleolin OS=Homo sapiens GN=NCL PE=1 SV=3	2
CALM	Calmodulin OS=Homo sapiens GN=CALM1 PE=1 SV=2	2
PTMA	Prothymosin alpha OS=Homo sapiens GN=PTMA PE=1 SV=2	2
PTMA	Isoform 2 of Prothymosin alpha OS=Homo sapiens GN=PTMA	2
SODC	Superoxide dismutase [Cu-Zn] OS=Homo sapiens GN=SOD1 PE=1 SV=2	2
PCBP2	Poly(rC)-binding protein 2 OS=Homo sapiens GN=PCBP2 PE=1 SV=1	2
ROAA	Isoform 3 of Heterogeneous nuclear ribonucleoprotein A/B OS=Homo sapiens GN=HNRNPAB	2
ROAA	Isoform 2 of Heterogeneous nuclear ribonucleoprotein A/B OS=Homo sapiens GN=HNRNPAB	2
SMD2	Small nuclear ribonucleoprotein Sm D2 OS=Homo sapiens GN=SNRPD2 PE=1 SV=1	2
HNRPM	Heterogeneous nuclear ribonucleoprotein M OS=Homo sapiens GN=HNRNPM PE=1 SV=3	2
HNRPM	Isoform 2 of Heterogeneous nuclear ribonucleoprotein M OS=Homo sapiens GN=HNRNPM	2
CF115	Costars family protein C6orf115 OS=Homo sapiens GN=C6orf115 PE=1 SV=1	2
ENPL	Endoplasmic OS=Homo sapiens GN=HSP90B1 PE=1 SV=1	2
HNRDL	Isoform 3 of Heterogeneous nuclear ribonucleoprotein D-like OS=Homo sapiens GN=HNRPDL	1
HNRDL	Isoform 2 of Heterogeneous nuclear ribonucleoprotein D-like OS=Homo sapiens GN=HNRPDL	1
HGB1A	Putative high mobility group protein B1-like 1 OS=Homo sapiens GN=HMGB1P1 PE=5 SV=1	1
SRSF7	Serine/arginine-rich splicing factor 7 OS=Homo sapiens GN=SRSF7 PE=1 SV=1	1
RL21	60S ribosomal protein L21 OS=Homo sapiens GN=RPL21 PE=1 SV=2	1

Table S1: SAR of thalidomide derivatives from the literature

Drug	Assay	Activity	IC50 (nM)	Notes	Ref
Thalidomide	Anti-angiogenesis "rabbit cornea"	High		36% Systemic delivery (5-OH?)	D'Amato et al 1994
EM-12 (pthalimide - =O)	Anti-angiogenesis "rabbit cornea"	High		42%	
Supidimide	Anti-angiogenesis "rabbit cornea"	None		0 Non-terataogenic but sedative	
Thalidomide	Anti-TNFalpha LPS assay	Low	200,000		Muller et al 1999
Thal 5-NH2	Anti-TNFalpha LPS assay	Low	100,000		
Thal 4-NH2				NO2 instead of NH2 abolishes	
("Pomalidomide"/"Actimid")	Anti-TNFalpha LPS assay	High		13 activity	
EM-12 4-NH2 ("Revimid")	Anti-TNFalpha LPS assay	Medium		100 No PDE4 inhibition	
Pomalidomide-alpha methyl	Anti-TNFalpha LPS assay	Medium		44	
S-Pomalidomide	Anti-TNFalpha LPS assay	High		3.9	
				Activity maybe due to residual S-	
R-Pomalidomide	Anti-TNFalpha LPS assay	Medium		94 isomer	
Thalidomide	NF-kB inhibition (p50/p65 nuclear translocation)	High	2040		de-Blanco et al 2007
Pomalidomide (4-NH2)	NF-kB inhibition (p50/p65 nuclear translocation)	High	1270		
5HPP-33 (phenyl, 5-OH)	NF-kB inhibition (p50/p65 nuclear translocation)	High	530	has 5-OH, phenyl-isopropanol instad of glutarimide	
5HPP-33-4-OH	NF-kB inhibition (p50/p65 nuclear translocation)	High	4950	NH2 substitution inactive	
Pthalimide-5-OH-phenyl-bromo	NF-kB inhibition (p50/p65 nuclear translocation)	High	430	Only Bromo gives activity, no Chloro or Flouro	
Thalidomide	Myeloma RPMI8226, IM9, U266 inhibition	Low	>100,000		Iguchi et al 2007
5HPP-33	Myeloma RPMI8226, IM9, U266 inhibition	High	1000-10,000		
Thalidomide	Myeolma MM.1S cell growth inhibition	Low	>100,000		Hideshima et al 2000
Pomalidomide	Myeolma MM.1S cell growth inhibition	High	100		
5HPP-33	Cell growth inhibition	High	5000-10000		Li et al 2006
Thalidomide	Cell growth inhibition	Low	>300,000		
Paclitaxel	Cell growth inhibition	High	17-31		
5HPP33	Cell growth inhibition of Hel60 cells	High	3000		Noguchi et al 2005
4APP33 (4-NH2)	Cell growth inhibition of Hel60 cells	Medium	6,000		
5APP33 (5-NH2)	Cell growth inhibition of Hel60 cells	Low	10,000		

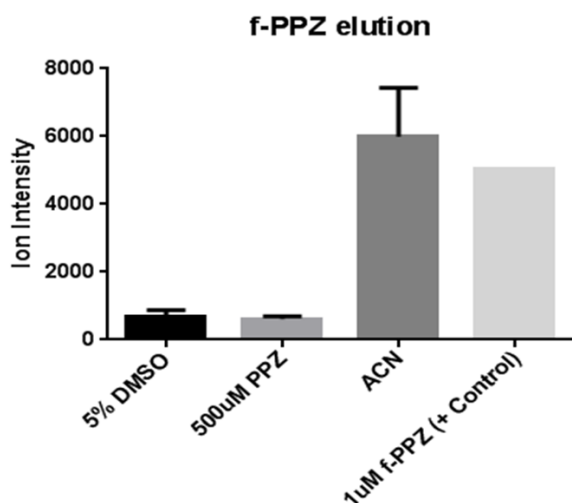


Figure S1: Proof-of-principle for elution of fluorous molecules with or without competing drug. We incubated 1uM of fluorous perphenazine with fluorous beads and eluted with DMSO, high-concentration competing perphenazine, or acetonitrile, and quantitated perphenazine recovery using LC-MS. Only acetonitrile led to recovery of perphenazine, at equal levels to 1uM perphenazine control in the LC-MS (far right).

References

- Aggarwal K, Choe LH, Lee KH. Shotgun proteomics using the iTRAQ isobaric tags. *Briefings in functional genomics & proteomics*. 2006;5(2):112-20.
- Ahn NG, Shabb JB, Old WM, Resing KA. Achieving in-depth proteomics profiling by mass spectrometry. *ACS Chem Biol*. 2007 01/01; 2013/02;2(1):39-52.
- Bajpai R, Chen DA, Rada-Iglesias A, Zhang J, Xiong Y, Helms J, Chang CP, Zhao Y, Swigut T, Wysocka J. CHD7 cooperates with PBAF to control multipotent neural crest formation. *Nature*. 2010 Feb 18;463(7283):958-62.
- Bantscheff M, Eberhard D, Abraham Y, Bastuck S, Boesche M, Hobson S, Mathieson T, Perrin J, Raida M, Rau C. Quantitative chemical proteomics reveals mechanisms of action of clinical ABL kinase inhibitors. *Nat Biotechnol*. 2007;25(9):1035-44.
- Barglow KT, Cravatt BF. Activity-based protein profiling for the functional annotation of enzymes. *Nature methods*. 2007;4(10):822-7.
- Bartlett J, Dredge K, Dalglish A. The evolution of thalidomide and its IMiD derivatives as anticancer agents. *Nature Reviews Cancer*. 2004;4:314.
- Bauer KS, Dixon SC, Figg WD. Inhibition of angiogenesis by thalidomide requires metabolic activation, which is species-dependent. *Biochem Pharmacol*. 1998 6/1;55(11):1827-34.
- Becher I, Savitski M, Faeltsh-Savitski M, Hopf C, Bantscheff M, Drewes G. Affinity profiling of the cellular kinome for the nucleotide cofactors ATP, ADP and GTP. *ACS Chemical Biology*. 2012
- Begley CG, Ellis LM. Drug development: Raise standards for preclinical cancer research. *Nature*. 2012;483(7391):531-3.
- Bredel M, Jacoby E. Chemogenomics: An emerging strategy for rapid target and drug discovery. *Nature Reviews Genetics*. 2004;5(4):262-75.
- Buchdunger E, Zimmermann J, Mett H, Meyer T, Müller M, Druker BJ, Lydon NB. Inhibition of the abl protein-tyrosine kinase in vitro and in vivo by a 2-phenylaminopyrimidine derivative. *Cancer Res*. 1996;56(1):100-4.
- Cepko C, Pear W. Overview of the retrovirus transduction system. *Curr Protoc Mol Biol*. 2001 May;Chapter 9:Unit9.9.
- Chamberlain PP, Lopez-Girona A, Miller K, Carmel G, Pagarigan B, Chie-Leon B, Rychak E, Corral LG, Ren YJ, Wang M. Structure of the human Cereblon–DDB1–lenalidomide complex reveals basis for responsiveness to thalidomide analogs. *Nature structural & molecular biology*. 2014

Christian MS, Laskin OL, Sharper V, Hoberman A, Stirling DI, Latriano L. Evaluation of the developmental toxicity of lenalidomide in rabbits. *Birth Defects Research Part B: Developmental and Reproductive Toxicology*. 2007;80(3):188-207.

Chung F, Lu J, Palmer BD, Kestell P, Browett P, Baguley BC, Tingle M, Ching L. Thalidomide pharmacokinetics and metabolite formation in mice, rabbits, and multiple myeloma patients. *Clinical Cancer Research*. 2004 September 01;10(17):5949-56.

Collins FS, Green ED, Guttmacher AE, Guyer MS. A vision for the future of genomics research. *Nature*. 2003;422(6934):835-47.

Corral LG, Kaplan G. Immunomodulation by thalidomide and thalidomide analogues. *Annals of the Rheumatic Diseases*. 1999 November 01;58(suppl 1):I107-13.

Cox J, Matic I, Hilger M, Nagaraj N, Selbach M, Olsen JV, Mann M. A practical guide to the MaxQuant computational platform for SILAC-based quantitative proteomics. *Nat Protoc*. 2009;4(5):698-705.

Cuatrecasas P. Protein purification by affinity chromatography. *J Biol Chem*. 1970;245(12):3059-65.

D'Amato RJ, Loughnan MS, Flynn E, Folkman J. Thalidomide is an inhibitor of angiogenesis. . - 4082 p.

Daub H, Godl K, Brehmer D, Klebl B, Müller G. Evaluation of kinase inhibitor selectivity by chemical proteomics. *Assay and drug development technologies*. 2004;2(2):215-24.

Dawson MA, Prinjha RK, Dittmann A, Giotopoulos G, Bantscheff M, Chan WI, Robson SC, Chung CW, Hopf C, Savitski MM, Huthmacher C, Gudgin E, Lugo D, Beinke S, Chapman TD, Roberts EJ, Soden PE, Auger KR, Mirguet O, Doehner K, Delwel R, Burnett AK, Jeffrey P, Drewes G, Lee K, Huntly BJ, Kouzarides T. Inhibition of BET recruitment to chromatin as an effective treatment for MLL-fusion leukaemia. *Nature*. 2011 Oct 2;478(7370):529-33.

Dobbs AP, Kimberley MR. Fluorous phase chemistry: A new industrial technology. *J Fluorine Chem*. 2002 12/1;118(1-2):3-17.

Drews J. Drug discovery: A historical perspective. *Science*. 2000;287(5460):1960-4.

Druker BJ, Tamura S, Buchdunger E, Ohno S, Segal GM, Fanning S, Zimmermann J, Lydon NB. Effects of a selective inhibitor of the abl tyrosine kinase on the growth of bcr-abl positive cells. *Nat Med*. 1996;2(5):561-6.

Eggert US, Kiger AA, Richter C, Perlman ZE, Perrimon N, Mitchison TJ, Field CM. Parallel chemical genetic and genome-wide RNAi screens identify cytokinesis inhibitors and targets. *PLoS biology*. 2004;2(12):e379.

Etchin J, Kanki JP, Look AT. Chapter 13 - Zebrafish as a Model for the Study of Human Cancer In: *Methods in Cell Biology*. Academic Press; p. 309-37.

Filippakopoulos P, Qi J, Picaud S, Shen Y, Smith WB, Fedorov O, Morse EM, Keates T, Hickman TT, Felletar I, Philpott M, Munro S, McKeown MR, Wang Y, Christie AL, West N, Cameron MJ, Schwartz B, Heightman TD, La Thangue N. Selective inhibition of BET bromodomains. *Nature*. 2010 12/23;468(7327):1067-73.

French CA, Ramirez CL, Kolmakova J, Hickman TT, Cameron MJ, Thyne ME, Kutok JL, Toretsky JA, Tadavarthy AK, Kees UR, Fletcher JA, Aster JC. BRD-NUT oncoproteins: A family of closely related nuclear proteins that block epithelial differentiation and maintain the growth of carcinoma cells. *Oncogene*. 2008 Apr 3;27(15):2237-42.

Frye SV. The art of the chemical probe. *Nat Chem Biol*. 2010 Mar;6(3):159-61.

Geitz H, Handt S, Zwingenberger K. Thalidomide selectively modulates the density of cell surface molecules involved in the adhesion cascade. *Immunopharmacology*. 1996;31(2-3):213.

Gladysz JA, Curran DP. Fluorous chemistry: From biphasic catalysis to a parallel chemical universe and beyond. *Tetrahedron*. 2002 5/13;58(20):3823-5.

Godl K, Gruss OJ, Eickhoff J, Wissing J, Blencke S, Weber M, Degen H, Brehmer D, Órfi L, Horváth Z. Proteomic characterization of the angiogenesis inhibitor SU6668 reveals multiple impacts on cellular kinase signaling. *Cancer Res*. 2005;65(15):6919-26.

Graves DJ, Wu YT. [10] on predicting the results of affinity procedures. *Meth Enzymol*. 1974;34:140-63.

Gregori-Puigjané E, Setola V, Hert J, Crews BA, Irwin JJ, Lounkine E, Marnett L, Roth BL, Shoichet BK. Identifying mechanism-of-action targets for drugs and probes. *Proceedings of the National Academy of Sciences*. 2012;109(28):11178-83.

Harding MW, Galat A, Uehling DE, Schreiber SL. A receptor for the immuno-suppressant FK 506 is a cis-trans peptidyl-prolyl isomerase. *Nature*. 1989;341(6244):758-60.

Heimann R, Ferguson D, Powers C, Recant WM, Weichselbaum RR, Hellman S. Angiogenesis as a Predictor of Long-term Survival for Patients With Node-Negative Breast Cancer. . - 1764 p.

Hert J, Irwin JJ, Laggner C, Keiser MJ, Shoichet BK. Quantifying biogenic bias in screening libraries. *Nature chemical biology*. 2009;5(7):479-83.

Hideshima T, Chauhan D, Shima Y, Raje N, Davies FE, Tai Y, Treon SP, Lin B, Schlossman RL, Richardson P, Muller G, Stirling DI, Anderson KC. Thalidomide and its analogs overcome drug resistance of human multiple myeloma cells to conventional therapy. *Blood*. 2000 November 01;96(9):2943-50.

Hoffmann, E. Mass spectrometry. Wiley Online Library; 2005.

Horrobin DF. Something rotten at the core of science? *Trends Pharmacol Sci*. 2001;22(2):51-2.

Horváth IT, Rábai J. Facile catalyst separation without water: Fluorous biphasic hydroformylation of olefins. *Science*. 1994 Oct. 7;266(5182):72-5.

Iguchi T, Yachide-Noguchi T, Hashimoto Y, Nakazato S, Sagawa M, Ikeda Y, Kizaki M. Novel tubulin-polymerization inhibitor derived from thalidomide directly induces apoptosis in human multiple myeloma cells: Possible anti-myeloma mechanism of thalidomide. *Int J Mol Med*. 2008 Feb;21(2):163-8.

Imming P, Sinning C, Meyer A. Drugs, their targets and the nature and number of drug targets. *Nature reviews Drug discovery*. 2006;5(10):821-34.

Ito T, Ando H, Suzuki T, Ogura T, Hotta K, Imamura Y, Yamaguchi Y, Handa H. Identification of a primary target of thalidomide teratogenicity. *Science*. 2010 March 12;327(5971):1345-50.

Jaeger S, Eriani G, Martin F. Results and prospects of the yeast three-hybrid system. *FEBS Lett*. 2004;556(1):7-12.

Kentsis A, Monigatti F, Dorff K, Campagne F, Bachur R, Steen H. Urine proteomics for profiling of human disease using high accuracy mass spectrometry. *PROTEOMICS ? Clinical Applications*. 2009;3(9):1052-61.

Kronke J, Udeshi ND, Narla A, Grauman P, Hurst SN, McConkey M, Svinkina T, Heckl D, Comer E, Li X, Ciarlo C, Hartman E, Munshi N, Schenone M, Schreiber SL, Carr SA, Ebert BL. Lenalidomide causes selective degradation of IKZF1 and IKZF3 in multiple myeloma cells. *Science*. 2014 Jan 17;343(6168):301-5.

Kuruvilla FG, Shamji AF, Sternson SM, Hergenrother PJ, Schreiber SL. Dissecting glucose signalling with diversity-oriented synthesis and small-molecule microarrays. *Nature*. 2002;416(6881):653-7.

Lacy MQ, Allred JB, Gertz MA, Hayman SR, Short KD, Buadi F, Dispenzieri A, Kumar S, Greipp PR, Lust JA, Russell SJ, Dingli D, Zeldenrust S, Fonseca R, Bergsagel PL, Roy V, Stewart AK, Laumann K, Mandrekar SJ, Reeder C, Rajkumar SV, Mikhael JR. Pomalidomide plus low-dose dexamethasone in myeloma refractory to both bortezomib and lenalidomide: Comparison of 2 dosing strategies in dual-refractory disease. *Blood*. 2011 Sep 15;118(11):2970-5.

Lacy MQ, Hayman SR, Gertz MA, Dispenzieri A, Buadi F, Kumar S, Greipp PR, Lust JA, Russell SJ, Dingli D, Kyle RA, Fonseca R, Bergsagel PL, Roy V, Mikhael JR, Stewart AK, Laumann K, Allred JB, Mandrekar SJ, Rajkumar SV. Pomalidomide (CC4047) plus low-dose dexamethasone as therapy for relapsed multiple myeloma. *J Clin Oncol*. 2009 Oct 20;27(30):5008-14.

Laggner C, Kokel D, Setola V, Tolia A, Lin H, Irwin JJ, Keiser MJ, Cheung CYJ, Minor Jr DL, Roth BL. Chemical informatics and target identification in a zebrafish phenotypic screen. *Nature Chemical Biology*. 2011;8(2):144-6.

Lovén J, Hoke HA, Lin CY, Lau A, Orlando DA, Vakoc CR, Bradner JE, Lee TI, Young RA. Selective inhibition of tumor oncogenes by disruption of super-enhancers. *Cell*. 2013;153(2):320-34.

Lu G, Middleton RE, Sun H, Naniang M, Ott CJ, Mitsiades CS, Wong KK, Bradner JE, Kaelin WG, Jr. The myeloma drug lenalidomide promotes the cereblon-dependent destruction of ikaros proteins. *Science*. 2014 Jan 17;343(6168):305-9.

Martinelli DC, Fan CM. The role of Gas1 in embryonic development and its implications for human disease. *Cell Cycle*. 2007 Nov 1;6(21):2650-5.

Matzuk M, McKeown M, Filippakopoulos P, Li Q, Ma L, Agno J, Lemieux M, Picaud S, Yu R, Qi J, Knapp S, Bradner J. Small-Molecule Inhibition of BRDT for Male Contraception. *Cell Press*; 2012. 673 p.

Meisner NC, Hintersteiner M, Uhl V, Weidemann T, Schmied M, Gstach H, Auer M. The chemical hunt for the identification of drugable targets. *Curr Opin Chem Biol*. 2004;8(4):424-31.

Miller RA, Chu Q, Xie J, Foretz M, Viollet B, Birnbaum MJ. Biguanides suppress hepatic glucagon signalling by decreasing production of cyclic AMP. *Nature*. 2013;494(7436):256-60.

Milne GM. . Pharmaceutical productivity—the imperative for new paradigms. *Annual Reports in Medicinal Chemistry*. 2003;38:383-96.

Miyachi H, Azuma A, Ogasawara A, Uchimura E, Watanabe N, Kobayashi Y, Kato F, Kato M, Hashimoto Y. Novel biological response modifiers: Phthalimides with tumor necrosis factor-alpha production-regulating activity. *J Med Chem*. 1997 Aug 29;40(18):2858-65.

Muller GW, Chen R, Huang SY, Corral LG, Wong LM, Patterson RT, Chen Y, Kaplan G, Stirling DI. Amino-substituted thalidomide analogs: Potent inhibitors of TNF-alpha production. *Bioorg Med Chem Lett*. 1999 Jun 7;9(11):1625-30.

Noguchi T, Miyachi H, Katayama R, Naito M, Hashimoto Y. Cell differentiation inducers derived from thalidomide. *Bioorg Med Chem Lett*. 2005 Jul 1;15(13):3212-5.

Ong SE, Blagoev B, Kratchmarova I, Kristensen DB, Steen H, Pandey A, Mann M. Stable isotope labeling by amino acids in cell culture, SILAC, as a simple and accurate approach to expression proteomics. *Molecular & Cellular Proteomics*. 2002;1(5):376-86.

Ott CJ, Kopp N, Bird L, Paranal RM, Qi J, Bowman T, Rodig SJ, Kung AL, Bradner JE, Weinstock DM. BET bromodomain inhibition targets both c-myc and IL7R in high-risk acute lymphoblastic leukemia. *Blood*. 2012 Oct 4;120(14):2843-52.

Overington JP, Al-Lazikani B, Hopkins AL. How many drug targets are there? *Nature reviews Drug discovery*. 2006;5(12):993-6.

Palumbo A, Gay F, Falco P, Crippa C, Montefusco V, Patriarca F, Rossini F, Caltagirone S, Benevolo G, Pescosta N, Guglielmelli T, Bringhen S, Offidani M, Giuliani N, Petrucci MT, Musto P, Liberati AM, Rossi G, Corradini P, Boccadoro M. Bortezomib as induction before autologous transplantation, followed by lenalidomide as consolidation-maintenance in untreated multiple myeloma patients. *Journal of Clinical Oncology*. 2010 February 10;28(5):800-7.

Palumbo A, Hajek R, Delforge M, Kropff M, Petrucci MT, Catalano J, Gisslinger H, Wiktor-Jędrzejczak W, Zodelava M, Weisel K, Cascavilla N, Iosava G, Cavo M, Kloczko J, Bladé J, Beksac M, Spicka I, Plesner T, Radke J, Langer C, Yehuda DB, Corso A, Herbein L, Yu Z, Mei J, Jacques C, Dimopoulos MA. Continuous lenalidomide treatment for newly diagnosed multiple myeloma. *N Engl J Med*. 2012 05/10; 2013/02;366(19):1759-69.

Price DK, Ando Y, Kruger EA, Weiss M, Figg WD. 5'-OH-thalidomide, a metabolite of thalidomide, inhibits angiogenesis. *Ther Drug Monit*. 2002 Feb;24(1):104-10.

Prinz F, Schlange T, Asadullah K. Believe it or not: How much can we rely on published data on potential drug targets? *Nature reviews Drug discovery*. 2011;10(9):712-.

Quintás-Cardama A, Kantarjian H, Cortes J. Flying under the radar: The new wave of BCR–ABL inhibitors. *Nature Reviews Drug Discovery*. 2007;6(10):834-48.

Rix U, Superti-Furga G. Target profiling of small molecules by chemical proteomics. *Nature chemical biology*. 2008;5(9):616-24.

Ross PL, Huang YN, Marchese JN, Williamson B, Parker K, Hattan S, Khainovski N, Pillai S, Dey S, Daniels S. Multiplexed protein quantitation in *saccharomyces cerevisiae* using amine-reactive isobaric tagging reagents. *Molecular & Cellular Proteomics*. 2004;3(12):1154-69.

Sabatini DM, Erdjument-Bromage H, Lui M, Tempst P, Snyder SH. RAFT1: A mammalian protein that binds to FKBP12 in a rapamycin-dependent fashion and is homologous to yeast TORs. *Cell*. 1994;78(1):35.

Sampaio EP, Sarno EN, Galilly R, Cohn ZA, Kaplan G. Thalidomide selectively inhibits tumor necrosis factor alpha production by stimulated human monocytes. *The Journal of Experimental Medicine*. 1991 March 01;173(3):699-703.

Savchuk NP, Balakin KV, Tkachenko SE. Exploring the chemogenomic knowledge space with annotated chemical libraries. *Curr Opin Chem Biol*. 2004;8(4):412-7.

Schreiber SL. Target-oriented and diversity-oriented organic synthesis in drug discovery. *Science*. 2000;287(5460):1964-9.

Schuffenhauer A, Floersheim P, Acklin P, Jacoby E. Similarity metrics for ligands reflecting the similarity of the target proteins. *J Chem Inf Comput Sci*. 2003;43(2):391-405.

Schug KA, Wang E, Shen S, Rao S, Smith SM, Hunt L, Mydlarz LD. Direct affinity screening chromatography-mass spectrometry assay for identification of antibacterial agents from natural product sources. *Anal Chim Acta*. 2011

Singhal S, Mehta J, Desikan R, Ayers D, Roberson P, Eddlemon P, Munshi N, Anaissie E, Wilson C, Dhodapkar M, Zeldis J, Siegel D, Crowley J, Barlogie B. Antitumor activity of thalidomide in refractory multiple myeloma. *N Engl J Med*. 1999 11/18; 2013/02;341(21):1565-71.

- Topaly J, Fruehauf S, Ho AD, Zeller WJ. Rationale for combination therapy of chronic myelogenous leukaemia with imatinib and irradiation or alkylating agents: Implications for pretransplant conditioning. *Br J Cancer*. 2002 May 6;86(9):1487-93.
- Vödösch M, Albrecht D, Leßing F, Schmidt AD, Winkler R, Guthke R, Brakhage AA, Kniemeyer O. Two-dimensional proteome reference maps for the human pathogenic filamentous fungus *aspergillus fumigatus*. *Proteomics*. 2009;9(5):1407-15.
- Wacker SA, Houghtaling BR, Elemento O, Kapoor TM. Using transcriptome sequencing to identify mechanisms of drug action and resistance. *Nature chemical biology*. 2012;8(3):235-7.
- Wilm M, Mann M. Analytical properties of the nanoelectrospray ion source. *Anal Chem*. 1996;68(1):1-8.
- Yang Y, Shaffer AL, Emre NT, Ceribelli M, Zhang M, Wright G, Xiao W, Powell J, Platig J, Kohlhammer H. Exploiting synthetic lethality for the therapy of ABC diffuse large B cell lymphoma. *Cancer cell*. 2012;21(6):723-37.
- Zhang W, Curran DP. Synthetic applications of fluorous solid-phase extraction (F-SPE). *Tetrahedron*. 2006 12/18;62(51):11837-65.
- Zhu YX, Braggio E, Shi C, Bruins LA, Schmidt JE, Van Wier S, Chang X, Bjorklund CC, Fonseca R, Bergsagel PL, Orlowski RZ, Stewart AK. Cereblon expression is required for the antimyeloma activity of lenalidomide and pomalidomide. *Blood*. 2011 November 03;118(18):4771-9.
- Zuber J, Shi J, Wang E, Rappaport AR, Herrmann H, Sison EA, Magoon D, Qi J, Blatt K, Wunderlich M, Taylor MJ, Johns C, Chicas A, Mulloy JC, Kogan SC, Brown P, Valent P, Bradner JE, Lowe SW, Vakoc CR. RNAi screen identifies Brd4 as a therapeutic target in acute myeloid leukaemia. *Nature*. 2011 Aug 3;478(7370):524-8.